ARTICLE

doi:10.1038/nature14132

New genetic loci link adipose and insulin biology to body fat distribution

A list of authors and their affiliations appears at the end of the paper

Body fat distribution is a heritable trait and a well-established predictor of adverse metabolic outcomes, independent of overall adiposity. To increase our understanding of the genetic basis of body fat distribution and its molecular links to cardiometabolic traits, here we conduct genome-wide association meta-analyses of traits related to waist and hip circumferences in up to 224,459 individuals. We identify 49 loci (33 new) associated with waist-to-hip ratio adjusted for body mass index (BMI), and an additional 19 loci newly associated with related waist and hip circumference measures ($P < 5 \times 10^{-8}$). In total, 20 of the 49 waist-to-hip ratio adjusted for BMI loci show significant sexual dimorphism, 19 of which display a stronger effect in women. The identified loci were enriched for genes expressed in adipose tissue and for putative regulatory elements in adipocytes. Pathway analyses implicated adipogenesis, angiogenesis, transcriptional regulation and insulin resistance as processes affecting fat distribution, providing insight into potential pathophysiological mechanisms.

Depot-specific accumulation of fat, particularly in the central abdomen, confers an increased risk of metabolic and cardiovascular diseases and mortality[1]. An easily accessible measure of body fat distribution is waist-to-hip ratio (WHR), a comparison of waist and hip circumferences. A larger WHR indicates more intra-abdominal fat deposition and is associated with higher risk for type 2 diabetes (T2D) and cardiovascular disease[2,3]. Conversely, a smaller WHR indicates greater gluteal fat accumulation and is associated with lower risk for T2D, hypertension, dyslipidemia and mortality[4–6]. Our previous genome-wide association study (GWAS) meta-analyses have identified loci for WHR after adjusting for body mass index (WHRadjBMI)[7,8]. These loci are enriched for association with other metabolic traits[7,8] and show that different fat distribution patterns can have distinct genetic components[9,10].

To determine further the genetic architecture of fat distribution and to increase our understanding of molecular connections with cardiometabolic traits, we performed a meta-analysis of WHRadjBMI associations in 142,762 individuals with GWAS data and 81,697 individuals genotyped with the Metabochip[11], all from the Genetic Investigation of ANthropometric Traits (GIANT) consortium. Given the marked sexual dimorphism previously observed among established WHRadjBMI loci[7,8], we performed analyses in men and women separately, the results of which were subsequently combined. To characterize the genetic determinants of specific aspects of body fat distribution more fully, we performed secondary GWAS meta-analyses for five additional traits: unadjusted WHR, unadjusted waist circumference, BMI-adjusted waist circumference (WCadjBMI), unadjusted hip circumference and BMI-adjusted hip circumference (HIPadjBMI). We evaluated the associated loci to understand their contributions to variation in fat distribution and adipose tissue biology, and their molecular links to cardiometabolic traits.

New loci associated with WHRadjBMI

We performed meta-analyses of GWAS of WHRadjBMI in up to 142,762 individuals of European ancestry from 57 new or previously described GWAS[7], and separately in up to an additional 67,326 European ancestry individuals from 44 Metabochip studies (Extended Data Fig. 1 and Supplementary Tables 1–3). The combination of these two meta-analyses included up to 2,542,447 autosomal single nucleotide polymorphisms (SNPs) in up to 210,088 European ancestry individuals. We defined new loci based on genome-wide significant association ($P < 5 \times 10^{-8}$ after genomic control correction at both the study-specific and meta-analytic levels) and distance (>500 kilobases (kb) from previously established loci)[7,8].

We identified 49 loci for WHRadjBMI, 33 of which were new and 16 previously described[7,8]. Of these, a European ancestry sex-combined analysis identified 39 loci, 24 of which were new[7,8] (Table 1, Supplementary Table 4 and Supplementary Figs 1–3). European ancestry sex-specific analyses identified nine additional loci, eight of which were new and significant in women but not in men (all $P_{men} > 0.05$; Table 1 and Supplementary Fig. 4). The addition of 14,371 individuals of non-European ancestry genotyped on the Metabochip identified one additional locus in women (rs1534696, near *SNX10*, $P_{women} = 2.1 \times 10^{-8}$, $P_{men} = 0.26$, Table 1 and Supplementary Tables 1–3), with no evidence of heterogeneity across ancestries ($P_{het} = 0.86$; Supplementary Note).

Genetic architecture of WHRadjBMI

To evaluate sexual dimorphism, we compared sex-specific effect size estimates of the 49 WHRadjBMI lead SNPs. The effect estimates were significantly different ($P_{difference} < 0.05/49 = 0.001$) at 20 SNPs, 19 of which showed larger effects in women (Table 1 and Extended Data Fig. 2a), similar to previous findings[7,8]. The only SNP that showed a larger effect in men mapped near *GDF5* (rs224333, $\beta_{men} = 0.036$ and $P = 9.0 \times 10^{-12}$, $\beta_{women} = 0.009$ and $P = 0.074$, $P_{difference} = 6.4 \times 10^{-5}$), a locus previously associated with height (rs6060369, $r^2 = 0.96$ and rs143384, $r^2 = 0.96$, 1000 Genomes Project CEU), although without significant differences between sexes[12,13]. Consistent with the larger number of loci identified in women, variance component analyses demonstrated a significantly larger heritability (h^2) of WHRadjBMI in women than men in the Framingham Heart Study ($h^2_{women} = 0.46$, $h^2_{men} = 0.19$, $P_{difference} = 0.0037$) and TwinGene study ($h^2_{women} = 0.56$, $h^2_{men} = 0.32$, $P_{difference} = 0.001$; Supplementary Table 5 and Extended Data Fig. 2b).

To identify multiple association signals within observed loci, we performed approximate conditional analyses of the sex-combined and sex-specific summary statistics using GCTA[14] (Supplementary Note). Several signals ($P < 5 \times 10^{-8}$) were identified at nine loci (Extended Data Table 1). Fitting SNPs jointly identified different lead SNPs in the sex-specific and sex-combined analyses. For example, the *MAP3K1-ANKRD55* locus showed near-independent (linkage disequilibrium (LD) $r^2 < 0.01$) SNPs 54 kb apart that were significant only in women

Table 1 | WHRadjBMI loci in sex-combined and sex-specific meta-analyses

					Sex-combined			Women			Men			Sex diff.
SNP	Chr	Locus	EA*	EAF	β	*P*	*N*	β	*P*	*N*	β	*P*	*N*	*P*†
Novel loci achieving genome-wide significance in European-ancestry meta-analyses														
rs905938	1	*DCST2*	T	0.74	0.025	7.3×10^{-10}	207,867	0.034	**4.9×10^{-10}**	115,536	0.015	1.1×10^{-2}	92,461	1.6×10^{-2}
rs10919388	1	*GORAB*	C	0.72	0.024	3.2×10^{-9}	181,049	0.033	**4.8×10^{-10}**	102,446	0.013	3.0×10^{-2}	78,738	9.8×10^{-3}
rs1385167	2	*MEIS1*	G	0.15	0.029	**1.9×10^{-9}**	206,619	0.023	4.0×10^{-4}	114,668	0.036	2.3×10^{-7}	92,085	1.6×10^{-1}
rs1569135	2	*CALCRL*	A	0.53	0.021	**5.6×10^{-10}**	209,906	0.023	6.9×10^{-7}	116,642	0.019	1.5×10^{-4}	93,398	5.8×10^{-1}
rs10804591	3	*PLXND1*	A	0.79	0.025	6.6×10^{-9}	209,921	0.040	**6.1×10^{-13}**	116,667	0.004	5.3×10^{-1}	93,387	**5.7×10^{-6}**
rs17451107	3	*LEKR1*	T	0.61	0.026	**1.1×10^{-12}**	207,795	0.023	1.0×10^{-6}	115,735	0.030	1.4×10^{-8}	92,194	3.5×10^{-1}
rs3805389	4	*NMU*	A	0.28	0.012	1.5×10^{-3}	209,218	0.027	**4.6×10^{-8}**	116,226	−0.007	2.1×10^{-1}	93,125	**1.6×10^{-6}**
rs9991328	4	*FAM13A*	T	0.49	0.019	4.5×10^{-8}	209,925	0.028	**3.4×10^{-10}**	116,652	0.007	1.7×10^{-1}	93,407	**8.5×10^{-4}**
rs303084	4	*SPATA5-FGF2*	A	0.80	0.023	**3.9×10^{-8}**	209,941	0.029	3.4×10^{-7}	116,662	0.016	9.9×10^{-3}	93,412	1.1×10^{-1}
rs9687846	5	*MAP3K1*	A	0.19	0.024	7.1×10^{-8}	208,181	0.041	**3.8×10^{-12}**	115,897	0.000	9.7×10^{-1}	92,417	**1.3×10^{-6}**
rs6556301	5	*FGFR4*	T	0.36	0.022	**2.6×10^{-8}**	178,874	0.018	7.1×10^{-4}	101,638	0.029	1.0×10^{-6}	77,370	1.4×10^{-1}
rs7759742	6	*BTNL2*	A	0.51	0.023	**4.4×10^{-11}**	208,263	0.024	1.7×10^{-7}	115,648	0.023	5.5×10^{-6}	92,749	8.6×10^{-1}
rs1776897	6	*HMGA1*	G	0.08	0.030	1.1×10^{-5}	177,879	0.052	**6.8×10^{-9}**	100,516	0.003	7.4×10^{-1}	77,497	**1.8×10^{-4}**
rs7801581	7	*HOXA11*	T	0.24	0.027	**3.7×10^{-10}**	195,215	0.025	7.7×10^{-6}	108,866	0.029	2.4×10^{-6}	86,483	6.9×10^{-1}
rs7830933	8	*NKX2-6*	A	0.77	0.022	7.4×10^{-8}	209,766	0.037	**1.2×10^{-12}**	116,567	0.001	8.4×10^{-1}	93,333	**1.4×10^{-6}**
rs12679556	8	*MSC*	G	0.25	0.027	**2.1×10^{-11}**	203,826	0.033	2.1×10^{-10}	114,369	0.017	4.2×10^{-3}	89,591	2.8×10^{-2}
rs10991437	9	*ABCA1*	A	0.11	0.031	**1.0×10^{-8}**	209,941	0.040	2.8×10^{-8}	116,644	0.022	6.1×10^{-3}	93,430	7.2×10^{-2}
rs7917772	10	*SFXN2*	A	0.62	0.014	5.6×10^{-5}	209,642	0.027	**5.5×10^{-9}**	116,514	−0.001	8.6×10^{-1}	93,263	**2.3×10^{-5}**
rs11231693	11	*MACROD1-VEGFB*	A	0.06	0.041	4.5×10^{-8}	198,072	0.068	**2.7×10^{-11}**	110,164	0.009	4.2×10^{-1}	88,043	**2.5×10^{-5}**
rs4765219	12	*CCDC92*	C	0.67	0.028	**1.6×10^{-15}**	209,807	0.037	1.0×10^{-14}	116,592	0.018	5.3×10^{-4}	93,350	5.7×10^{-3}
rs8042543	15	*KLF13*	C	0.78	0.026	**1.2×10^{-9}**	208,255	0.023	6.7×10^{-5}	115,760	0.030	1.0×10^{-6}	92,629	3.6×10^{-1}
rs8030605	15	*RFX7*	A	0.14	0.030	**8.8×10^{-9}**	208,374	0.031	1.0×10^{-5}	115,864	0.031	5.9×10^{-5}	92,644	9.9×10^{-1}
rs1440372	15	*SMAD6*	C	0.71	0.024	**1.1×10^{-10}**	207,447	0.022	1.1×10^{-5}	115,201	0.027	1.4×10^{-6}	92,380	5.2×10^{-1}
rs2925979	16	*CMIP*	T	0.31	0.018	1.2×10^{-6}	207,828	0.032	**3.4×10^{-11}**	115,431	−0.002	7.9×10^{-1}	92,531	**1.2×10^{-6}**
rs4646404	17	*PEMT*	G	0.67	0.027	**1.4×10^{-11}**	198,196	0.034	5.3×10^{-11}	115,337	0.017	2.5×10^{-3}	87,857	2.6×10^{-2}
rs8066985	17	*KCNJ2*	A	0.50	0.018	1.4×10^{-7}	209,977	0.026	**4.0×10^{-9}**	116,683	0.007	1.9×10^{-1}	93,428	1.8×10^{-3}
rs12454712	18	*BCL2*	T	0.61	0.016	1.0×10^{-4}	169,793	0.035	**1.1×10^{-9}**	96,182	−0.007	2.5×10^{-1}	73,576	**1.6×10^{-7}**
rs12608504	19	*JUND*	A	0.36	0.022	**8.8×10^{-10}**	209,990	0.017	2.6×10^{-4}	116,689	0.028	1.1×10^{-7}	93,435	1.2×10^{-1}
rs4081724	19	*CEBPA*	G	0.85	0.035	**7.4×10^{-12}**	207,418	0.033	9.2×10^{-7}	115,322	0.039	1.4×10^{-7}	92,230	5.0×10^{-1}
rs979012	20	*BMP2*	T	0.34	0.027	**3.3×10^{-14}**	209,941	0.026	1.0×10^{-7}	116,668	0.028	6.6×10^{-8}	93,407	6.7×10^{-1}
rs224333	20	*GDF5*	G	0.62	0.020	2.6×10^{-8}	208,025	0.009	7.4×10^{-2}	115,803	0.036	**9.0×10^{-12}**	92,356	**6.4×10^{-5}**
rs6090583	20	*EYA2*	A	0.48	0.022	**6.2×10^{-11}**	209,435	0.029	2.8×10^{-10}	116,382	0.015	2.4×10^{-3}	93,187	3.2×10^{-2}
Novel loci achieving genome-wide significance in all-ancestry meta-analyses														
rs1534696	7	*SNX10*	C	0.43	0.011	1.3×10^{-3}	212,501	0.027	**2.1×10^{-8}**	118,187	−0.006	2.6×10^{-1}	92,243	**2.1×10^{-6}**
Previously reported loci achieving genome-wide significance in European-ancestry meta-analyses														
rs2645294	1	*TBX15-WARS2*	T	0.58	0.031	**1.7×10^{-19}**	209,808	0.035	1.5×10^{-14}	116,596	0.027	1.5×10^{-7}	93,346	2.0×10^{-1}
rs714515	1	*DNM3-PIGC*	G	0.43	0.027	**4.4×10^{-15}**	203,401	0.029	1.8×10^{-10}	113,939	0.025	8.5×10^{-7}	89,596	5.1×10^{-1}
rs2820443	1	*LYPLAL1*	T	0.72	0.035	5.3×10^{-21}	209,975	0.062	**5.7×10^{-35}**	116,672	0.002	6.9×10^{-1}	93,437	**2.6×10^{-17}**
rs10195252	2	*GRB14-COBLL1*	T	0.59	0.027	5.9×10^{-15}	209,395	0.052	**4.7×10^{-30}**	116,329	−0.003	5.3×10^{-1}	93,199	**2.4×10^{-17}**
rs17819328	3	*PPARG*	G	0.43	0.021	2.4×10^{-9}	208,809	0.035	**4.6×10^{-14}**	116,072	0.005	3.3×10^{-1}	92,871	**5.1×10^{-6}**
rs2276824	3	*PBRM1*‡	C	0.43	0.024	**3.2×10^{-11}**	208,901	0.028	3.7×10^{-9}	116,128	0.020	1.4×10^{-4}	92,907	2.0×10^{-1}
rs2371767	3	*ADAMTS9*	G	0.72	0.036	1.6×10^{-20}	194,506	0.056	**1.2×10^{-26}**	108,624	0.012	3.5×10^{-2}	86,016	**3.6×10^{-9}**
rs1045241	5	*TNFAIP8-HSD17B4*	C	0.71	0.019	4.4×10^{-7}	209,710	0.035	**6.6×10^{-12}**	116,560	−0.001	9.3×10^{-1}	93,284	**8.3×10^{-7}**
rs7705502	5	*CPEB4*	A	0.33	0.027	**4.7×10^{-14}**	209,827	0.027	1.9×10^{-8}	116,609	0.027	2.3×10^{-7}	93,352	>0.99
rs1294410	6	*LY86*	C	0.63	0.031	**2.0×10^{-18}**	209,830	0.037	1.6×10^{-15}	116,624	0.025	1.4×10^{-6}	93,340	6.3×10^{-2}
rs1358980	6	*VEGFA*	T	0.47	0.039	3.1×10^{-27}	206,862	0.060	**3.7×10^{-34}**	115,047	0.015	4.0×10^{-3}	91,949	**3.7×10^{-11}**
rs1936805	6	*RSPO3*	T	0.51	0.043	**3.6×10^{-35}**	209,859	0.052	3.7×10^{-30}	116,602	0.031	3.1×10^{-10}	93,392	**1.0×10^{-3}**
rs10245353	7	*NFE2L3*	A	0.20	0.035	**8.4×10^{-16}**	210,008	0.041	7.9×10^{-13}	116,704	0.027	1.4×10^{-5}	93,438	7.2×10^{-2}
rs10842707	12	*ITPR2-SSPN*	T	0.23	0.032	**4.4×10^{-16}**	210,023	0.041	6.1×10^{-15}	116,704	0.022	1.4×10^{-4}	93,453	1.1×10^{-2}
rs1443512	12	*HOXC13*	A	0.24	0.028	6.9×10^{-13}	209,980	0.040	**1.1×10^{-14}**	116,688	0.013	2.8×10^{-2}	93,425	**1.6×10^{-4}**
rs2294239	22	*ZNRF3*	A	0.59	0.025	**7.2×10^{-13}**	209,454	0.028	6.9×10^{-10}	116,414	0.024	2.3×10^{-6}	93,173	5.0×10^{-1}

Loci achieving genome-wide significance ($P < 5\times10^{-8}$) in sex-combined and/or sex-specific meta-analyses. *P* values and β coefficients for the association with WHRadjBMI in the meta-analyses of combined GWAS and Metabochip studies. The smallest *P* value for each SNP is shown in bold. Chr, chromosome; EAF, effect allele frequency.

* The effect allele (EA) is the WHRadjBMI-increasing allele in the sex-combined analysis.

† Test for sex difference; values significant at the table-wise Bonferroni threshold of $0.05/49 = 1.02\times10^{-3}$ are marked in bold.

‡ Locus previously named *NISCH-STAB1*. Additional analyses that showed no significant evidence of heterogeneity between studies or due to ascertainment are provided in Supplementary Tables 27 and 28 (Supplementary Note).

(rs3936510) or only in men (rs459193; Extended Data Table 1, Supplementary Table 4). Other signals are more complex. The *TBX15-WARS2* locus showed different but correlated lead SNPs in men and women near *WARS2* ($r^2 = 0.43$), an independent signal near *TBX15*, and a distant independent signal near *SPAG17* (Fig. 1). At the *HOXC* gene cluster, conditional analyses identified independent ($r^2 < 0.01$) SNPs ~80 kb apart near *HOXC12-HOXC13-HOTAIR* and near *HOXC4-HOXC6* (Fig. 1). These results suggest that association signals mapping to the same locus might act on different underlying genes and may not be relevant to the same sex.

We assessed the aggregate effects of the primary association signals at the 49 WHRadjBMI loci by calculating sex-combined and sex-specific risk based on genotypes of the lead SNPs. In a linear regression model, the risk scores were associated with WHRadjBMI, with a stronger effect in women than in men (overall effect per allele $\beta = 0.001$, $P = 6.7\times10^{-4}$, women $\beta = 0.002$, $P = 1.0\times10^{-11}$, men $\beta = 7.0\times10^{-4}$, $P = 0.02$;

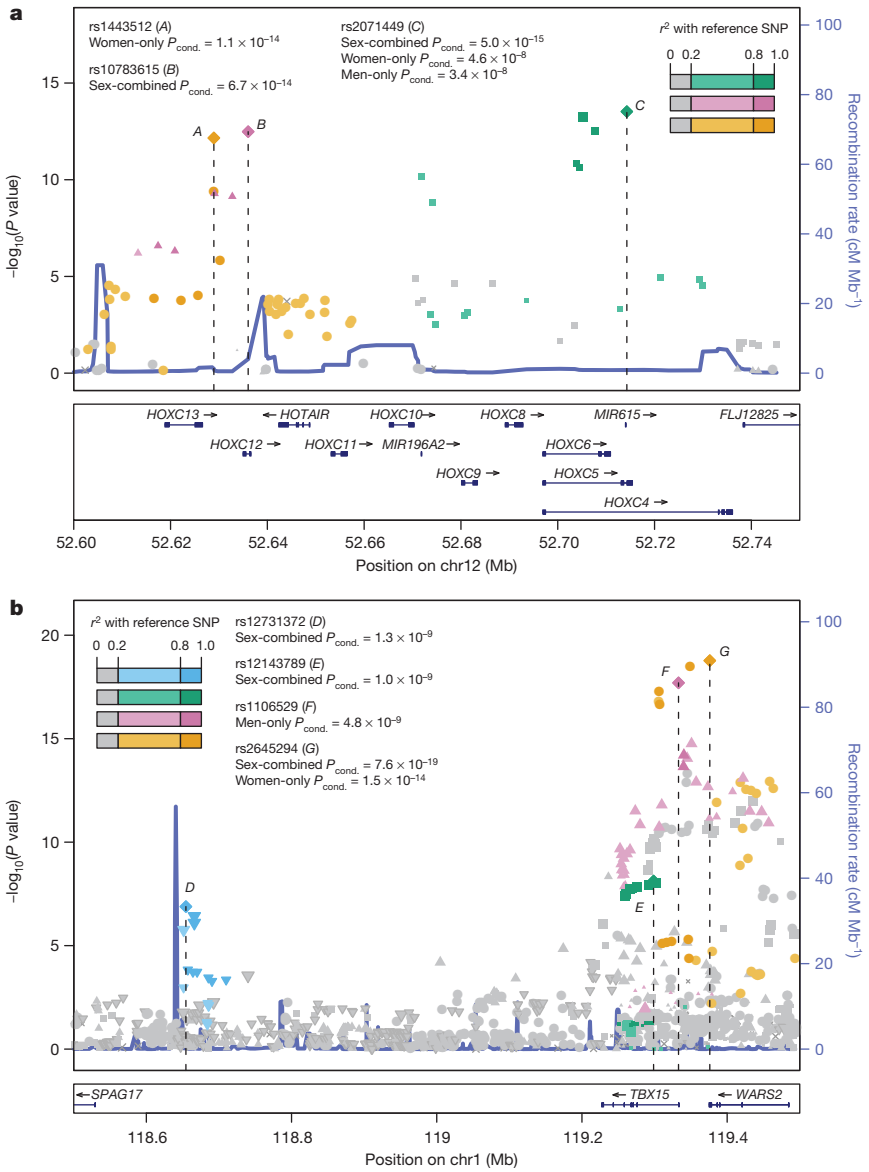

Figure 1 | Regional SNP association plots illustrating the complex genetic architecture at two WHRadjBMI loci. **a**, **b**, Sex-combined meta-analysis SNP associations in European individuals were plotted with $-\log_{10}$ *P* values (left *y* axis) and estimated local recombination rate in blue (right *y* axis). Three index SNPs near *HOXC6-HOXC13* (denoted *A*–*C*) (**a**) and four near *TBX15-WARS2-SPAG17* (*D*–*G*) (**b**) were identified through approximate conditional analyses of sex-combined or sex-specific associations (values shown as $P_{conditional} < 5 \times 10^{-8}$, see Methods). The signals are distinguished by both colour and shape, and linkage disequilibrium (r^2) of nearby SNPs is shown by colour intensity gradient. Sample sizes for the index SNP associations are listed in Extended Data Table 1.

Extended Data Fig. 3 and Supplementary Note). The 49 SNPs explained 1.4% of the variance in WHRadjBMI overall, and more in women (2.4%) than in men (0.8%) (Supplementary Table 6). Compared to the 16 previously reported loci[7,8], the new loci almost doubled the explained variance in women and tripled that in men. We further estimated that the sex-combined variance explained by all HapMap SNPs[15] (h^2_G) is 12.1% (s.e.m. = 2.9%).

At 17 loci with high-density coverage on the Metabochip[11], we used association summary statistics to define credible sets of SNPs with a high probability of containing a likely functional variant. The 99% credible sets at seven loci spanned <20 kb, and at *HOXC13* included only a single noncoding SNP (Supplementary Table 7 and Supplementary Fig. 5). Imputation up to higher density reference panels will provide greater coverage and may have more potential to localize functional variants.

WHRadjBMI variants and other traits

Given the epidemiological correlations between central obesity and other anthropometric and cardiometabolic measures and diseases, we evaluated lead WHRadjBMI variants in association data from GWAS consortia for 22 traits. In total, 17 of the 49 variants were associated ($P < 5 \times 10^{-8}$) with at least one of the traits: high-density lipoprotein cholesterol (HDL; $n = 7$ SNPs), triglycerides ($n = 5$), low-density lipoprotein cholesterol (LDL; $n = 2$), adiponectin adjusted for BMI ($n = 3$), fasting insulin adjusted for BMI ($n = 2$), T2D ($n = 1$), and height ($n = 7$) (Supplementary Tables 8 and 9). WHRadjBMI SNPs also showed enrichment for directional consistency among nominally significant ($P < 0.05$) associations with these traits and also with fasting and 2-h glucose, diastolic and systolic blood pressure, BMI and coronary artery disease (CAD) ($P_{binomial} < 0.05/23 = 0.0022$; Extended Data Table 2); these results were generally supported by meta-regression analysis of the regression coefficient estimates (Supplementary Table 10). Furthermore, our WHRadjBMI loci overlap with associations reported in the National Human Genome Research Institute (NHGRI) GWAS catalogue (Table 2 and Supplementary Table 11)[16], the strongest of which is the locus near *LEKR1*, which is associated ($P = 2.0 \times 10^{-35}$) with birth weight[17]. Unsupervised hierarchical clustering of the corresponding matrix of association *Z*-scores showed three major clusters characterized by patterns of anthropometric and metabolic traits (Extended Data Fig. 4). These data extend knowledge about genetic links between WHRadjBMI and insulin-resistance-related traits; whether this reflects underlying causal relations between WHRadjBMI and these traits, or pleiotropic loci, cannot be inferred from our data.

Potential functional WHRadjBMI variants

We next examined variants in LD with the WHRadjBMI lead SNPs ($r^2 > 0.7$) for predicted effects on protein sequence, copy number, and

Table 2 | Candidate genes at new WHRadjBMI loci

SNP	Locus	eQTL ($P < 10^{-5}$)*	GRAIL ($P < 0.05$)†	DEPICT (FDR < 0.05)‡	Literature§	Other GWAS signals‖
rs905938	*DCST2*	*ZBTB7B* (PB, blood)	-	-	-	-
rs10919388	*GORAB*	-	-	-	-	-
rs1385167	*MEIS1*	-	-	-	*MEIS1*	-
rs1569135	*CALCRL*	-	*TFPI*	-	*CALCRL*	-
rs10804591	*PLXND1*	-		-	*PLXND1*	-
rs17451107	*LEKR1*	*TIPARP* (S,O), *LEKR1* (S)		-	-	Birth weight: *CCNL1*, *LEKR1*
rs3805389	*NMU*	-	-	-	*NMU*	-
rs9991328	*FAM13A*	*FAM13A* (S)		*FAM13A*	-	FI: *FAM13A*
rs303084	*SPATA5-FGF2*	-	*FGF2*	-	*FGF2*, *NUDT6*, *SPRY1*	-
rs9687846	*MAP3K1*	-	*MAP3K1*	-	*MAP3K1*	FI, TG: *ANKRD55*, *MAP3K1*
rs6556301	*FGFR4*	-	*MXD3*	-	*FGFR4*	Height
rs7759742	*BTNL2*	*HLA-DRA* (S), *KLHL31* (S)	-	(not analysed)	-	-
rs1776897	*HMGA1*	-	-	(not analysed)	*HMGA1*	Height: *HMGA1*, *C6orf106*, *LBH*
rs1534696	*SNX10*	*SNX10* (S), *CBX3* (S)	-	-	*SNX10*	-
rs7801581	*HOXA11*	-	*HOXA11*	*HOXA11*	*HOXA11*	-
rs7830933	*NKX2-6*	*STC1* (S)	-	-	*NKX2-6*, *STC1*	-
rs12679556	*MSC*	-	*EYA1*	*RP11-1102P16.1*	*MSC*, *EYA1*	-
rs10991437	*ABCA1*	-		-	*ABCA1*	-
rs7917772	*SFXN2*	-	-	-	*SFXN2*	Height
rs11231693	*MACROD1-VEGFB*	-	*VEGFB*	*MACROD1*	*MACROD1*, *VEGFB*	-
rs4765219	*CCDC92*	*CCDC92* (S, O, L), *ZNF664* (S, O)	*FAM101A*	-	-	Adiponectin, FI, HDL, TG: *CCDC92*, *ZNF664*
rs8042543	*KLF13*	-	*KLF13*	-	*KLF13*	-
rs8030605	*RFX7*	-		-	-	-
rs1440372	*SMAD6*	*SMAD6* (blood)	*SMAD6*	*SMAD6*	*SMAD6*	Height
rs2925979	*CMIP*	*CMIP* (S)	-	-	*CMIP*, *PLCG2*	Adiponectin, FI, HDL: *CMIP*
rs4646404	*PEMT*	-	-	*PEMT*	*PEMT*	-
rs8066985	*KCNJ2*	-	-	-	*KCNJ2*	-
rs12454712	*BCL2*	-	-	-	*BCL2*	-
rs12608504	*JUND*	*KIAA1683* (PB, O), *JUND* (LCL)	*JUND*	-	*JUND*	-
rs4081724	*CEBPA*	-	*CEBPA*	-	*CEBPA*, *CEBPG*	-
rs979012	*BMP2*	-	*BMP2*	*BMP2*	*BMP2*	Height: *BMP2*
rs224333	*GDF5*	*CEP250* (S, O), *UQCC* (blood, S, O, L, LCL)	*GDF5*	*GDF5*	*GDF5*	Height: *GDF5*, *UQCC*
rs6090583	*EYA2*	-	*EYA2*	*EYA2*	*EYA2*	-

Candidate genes based on secondary analyses or literature review. Details are provided in Supplementary Tables 8, 9, 11–13, 15, 19, 21 and Supplementary Note. The only non-synonymous variant in high LD with an index SNP was *GDF5* S276A. No copy number variants were identified. PB, peripheral blood mononuclear cells; FI, fasting insulin adjusted for BMI; HDL, high-density lipoprotein cholesterol; L, liver; LCL, lymphoblastoid cell line; O, omental adipose; S, subcutaneous adipose; TG, triglycerides.

* Gene transcript levels associated with the SNP in the indicated tissue(s).

† Genes in pathways identified as enriched by GRAIL analysis.

‡ Significant (FDR < 5%) pathway genes derived by DEPICT using GWAS-only results.

§ Most plausible candidate genes based on literature review.

‖ Traits associated at $P < 5 \times 10^{-8}$ in GWAS or the GWAS catalogue using the index SNP or a proxy, and the genes(s) named.

cis-regulatory effects on expression (Table 2, Supplementary Tables 12–15 and Supplementary Note). At 11 of the new loci, lead WHRadjBMI SNPs were in LD with *cis*-expression quantitative trait loci (eQTLs) for transcripts in subcutaneous adipose tissue, omental adipose tissue, liver or blood cell types (Table 2 and Supplementary Table 15). No additional sex-specific eQTLs were identified, perhaps reflecting limited power (Supplementary Table 16).

At the 11 WHRadjBMI loci containing eQTLs, we compared the location of the candidate variants to regions of open chromatin (DNase I hypersensitivity and formaldehyde-assisted isolation of regulatory elements (FAIRE)) and histone modification enrichment (histone 3 Lys 4 methylation (H3K4me1), H3K4me2, H3K4me3, histone 3 Lys 27 acetylation (H3K27ac), and H3K9ac) in adipose, liver, skeletal muscle, bone, brain, blood and pancreatic islet tissues or cell lines (Supplementary Table 17). At 7 of these 11 loci, at least one variant was located in a putative regulatory element in two or more data sets from the same tissue as the eQTL, suggesting that these elements may influence transcriptional activity (Supplementary Table 18). For example, at *LEKR1*, five variants in LD with the WHRadjBMI lead SNP are located in a 1.1-kb region with evidence of enhancer activity (H3K4me1 and H3K27ac) in adipose tissue (Extended Data Fig. 5a).

We also examined whether any variants overlapped with open chromatin or histone modifications from only one of the tested tissues, possibly reflecting tissue-specific regulatory elements (Supplementary Table 18). For example, five variants in a 2.2-kb region, located 77 kb upstream from a *CALCRL* transcription start site, overlapped with peaks in at least five data sets in endothelial cells (Extended Data Fig. 5b), suggesting that one or more of these variants may influence transcriptional activity. *CALCRL*, which is expressed in endothelial cells, is required for lipid absorption in the small intestine, and influences body weight in mice[18]. Other variants located in tissue-specific regulatory elements were detected at *NMU* for endothelial cells, at *KLF13* and *MEIS1* for liver, and at *GORAB* and *MSC* for bone (Supplementary Table 18).

Biological mechanisms

To identify potential functional connections between genes mapping to the 49 WHRadjBMI loci, we used three approaches (Supplementary Note). A survey of literature using GRAIL[19] identified 15 genes with nominal significance ($P < 0.05$) for potential functional connectivity (Table 2 and Supplementary Table 19). The predefined gene set relationships across loci identified using MAGENTA[20] highlighted signalling pathways involving vascular endothelial growth factor (VEGF), phosphatase and tensin (PTEN) homologue, the insulin receptor, and peroxisome proliferator-activated receptors (Supplementary Table 20). VEGF signalling plays a central, complex role in angiogenesis, insulin resistance and obesity[21], and PTEN signalling promotes insulin resistance[22]. Analyses using Data-driven Expression Prioritized Integration for Complex Traits (DEPICT)[23] facilitated prioritization of genes at associated loci, analyses of tissue specificity, and enrichment of reconstituted gene sets through integration of association results with expression data, protein–protein interactions, phenotypic data from gene knockout studies in mice, and predefined gene sets. DEPICT identified at least one

prioritized gene (false discovery rate (FDR) < 5%) at nine loci (Table 2 and Supplementary Table 21) and identified 234 reconstituted gene sets (161 after pruning of overlapping gene sets) enriched for genes at WHRadjBMI loci. Among these we highlight biologically plausible gene sets suggesting roles in body fat regulation (including adiponectin signalling, insulin sensitivity and regulation of glucose levels), skeletal growth, transcriptional regulation and development (Fig. 2 and Supplementary Table 22). We also note gene sets that are specific for abundance or development of metabolically active tissues including adipose, heart, liver and muscle. Specific genes at the loci were significantly enriched (FDR < 5%) for expression in adipocyte-related tissues, including abdominal subcutaneous fat (Fig. 2 and Supplementary Table 23). Together, these analyses identified processes related to insulin and adipose biology and highlight mesenchymal tissues, especially adipose tissue, as important to WHRadjBMI.

We also tested variants at the 49 WHRadjBMI loci for overlap with elements from 60 selected regulatory data sets from the ENCODE[24] and Epigenomic RoadMap[25] data and found evidence of enrichment in 12 data sets ($P < 0.05/60 = 8.3 \times 10^{-4}$; Extended Data Table 3). The strongest enrichments were detected for data sets typically attributed to enhancer activity (H3K4me1 and H3K27ac) in adipose, muscle, endothelial cells, and bone, suggesting that variants may regulate transcription in these tissues. These analyses point to mechanisms linking WHRadjBMI loci to regulation of gene expression in tissues highly relevant for adipocyte metabolism and insulin resistance.

We also reviewed functions of candidate genes located near new and previously established WHRadjBMI loci[7,8], identifying genes involved in adipogenesis, angiogenesis and transcriptional regulation (Table 2, literature review in the Supplementary Note). Adipogenesis candidate genes include *CEBPA*, *PPARG*, *BMP2*, *HOXC-mir196*, *SPRY1*, *TBX15*, and *PEMT*. Of these, *CEBPA* and *PPARG* are essential for white adipose tissue differentiation[26], *BMP2* induces differentiation of mesenchymal stem cells towards adipogenesis or osteogenesis[27], and *HOXC8* is a repressor of brown adipogenesis in mice that is regulated by miR-196a (ref. 28), also located within the *HOXC* region (Fig. 1). Angiogenesis genes may influence expansion and loss of adipose tissue[29]; they include *VEGFA*, *VEGFB*, *RSPO3*, *STAB1*, *WARS2*, *PLXND1*, *MEIS1*, *FGF2*, *SMAD6* and *CALCRL*. *VEGFB* is involved in endothelial targeting of lipids to peripheral tissues[30], and *PLXND1* limits blood vessel branching, antagonizes VEGF, and affects adipose inflammation[31,32]. Transcriptional regulators at WHRadjBMI loci include *CEBPA*, *PPARG*, *MSC*, *SMAD6*, *HOXA*, *HOXC*, *ZBTB7B*, *JUND*, *KLF13*, *MEIS1*, *RFX7*, *NKX2-6* and *HMGA1*. Other candidate genes include *NMU*, *FGFR4* and *HMGA1*, for which mice deficient for the corresponding genes exhibit obesity, glucose intolerance and/or insulin resistance[33–35].

Five additional central obesity traits

To determine whether the WHRadjBMI variants exert their effects primarily through waist circumference or hip circumference and to identify loci that are not reported for WHRadjBMI, BMI or height[36,37], we performed association analyses for five additional traits: WCadjBMI, HIPadjBMI, WHR, waist circumference and hip circumference. On the basis of phenotypic data alone, waist circumference and hip circumference are highly correlated with BMI ($r = 0.59$–0.92), and WHR is highly correlated with WHRadjBMI ($r = 0.82$–0.95), while WCadjBMI and HIPadjBMI are moderately correlated with height ($r = 0.24$–0.63; Supplementary Table 24). In contrast to WHRadjBMI, which has almost no genetic correlation (see Methods) with height ($r_G < 0.04$; Extended Data Fig. 2c), WCadjBMI ($r_G = 0.42$) and HIPadjBMI ($r_G = 0.82$) have moderate genetic correlations with height. These data suggest that some, but not all, WCadjBMI and HIPadjBMI loci would be associated with height.

Across all meta-analyses, we identified an additional 19 loci associated with one of the five traits ($P < 5 \times 10^{-8}$), nine of which showed

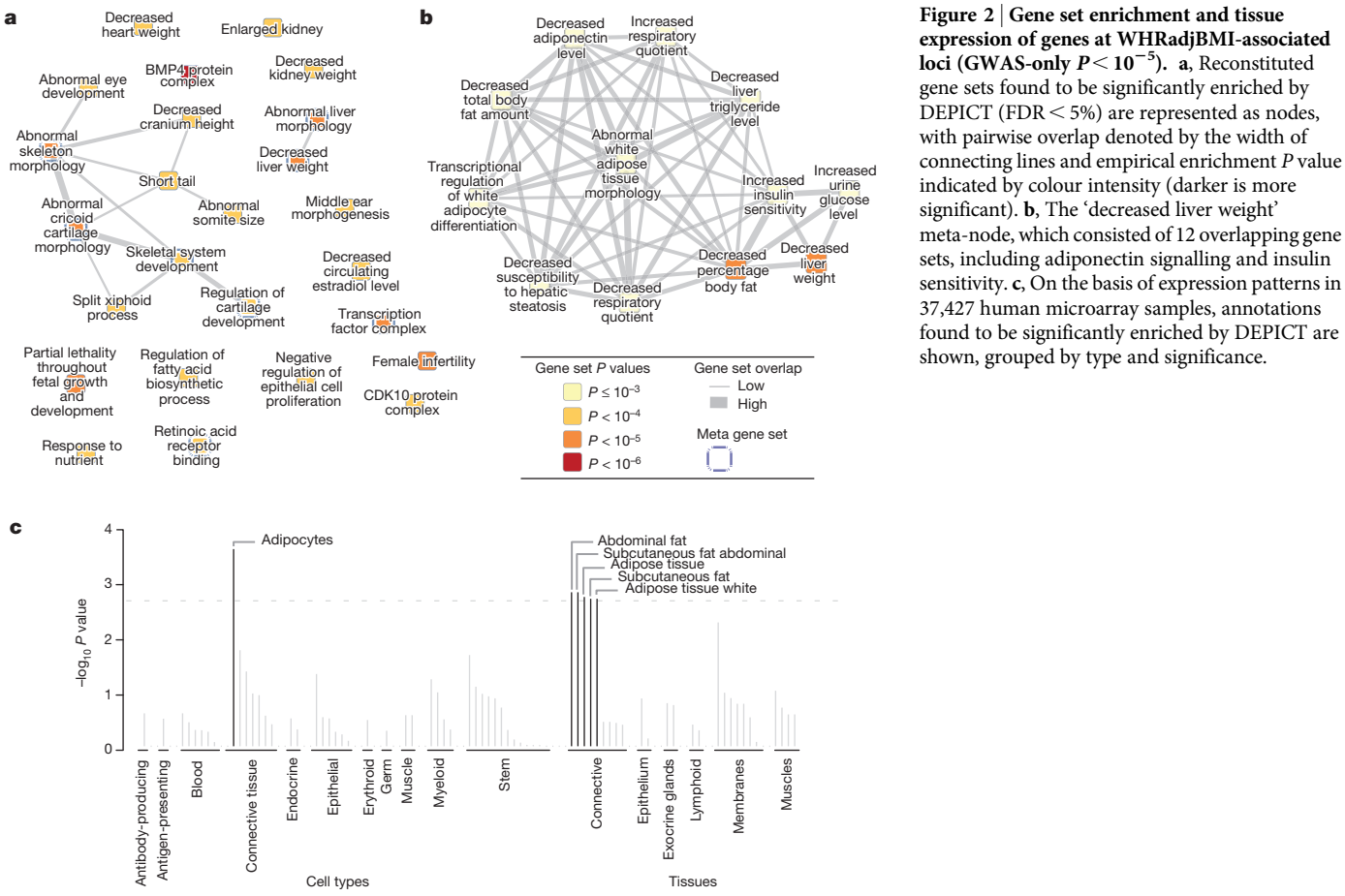

Figure 2 | Gene set enrichment and tissue expression of genes at WHRadjBMI-associated loci (GWAS-only $P < 10^{-5}$). **a**, Reconstituted gene sets found to be significantly enriched by DEPICT (FDR < 5%) are represented as nodes, with pairwise overlap denoted by the width of connecting lines and empirical enrichment *P* value indicated by colour intensity (darker is more significant). **b**, The 'decreased liver weight' meta-node, which consisted of 12 overlapping gene sets, including adiponectin signalling and insulin sensitivity. **c**, On the basis of expression patterns in 37,427 human microarray samples, annotations found to be significantly enriched by DEPICT are shown, grouped by type and significance.

Table 3 | New loci achieving genome-wide evidence of association ($P < 5 \times 10^{-8}$) with additional waist and hip circumference traits

						Sex-combined			Women			Men			Sex diff.
SNP	Trait	Chr	Locus	EA*	EAF	β	*P*	*N*	β	*P*	*N*	β	*P*	*N*	*P*†
Loci achieving genome-wide significance in European-ancestry meta-analyses															
rs10925060	WCadjBMI	1	*OR2W5-NLRP3*	T	0.03	0.017	2.2×10^{-5}	140,515	0.002	6.8×10^{-1}	85,186	0.045	**9.1×10^{-13}**	55,522	**1.7×10^{-8}**
rs10929925	HIP	2	*SOX11*	C	0.55	0.020	**4.5×10^{-8}**	207,648	0.021	9.0×10^{-6}	115,428	0.018	3.2×10^{-4}	92,499	6.1×10^{-1}
rs2124969	WCadjBMI	2	*ITGB6*	C	0.42	0.020	**7.1×10^{-9}**	231,284	0.016	3.5×10^{-4}	127,437	0.025	2.3×10^{-7}	104,039	1.4×10^{-1}
rs17472426	WCadjBMI	5	*CCNJL*	T	0.92	0.014	3.1×10^{-2}	217,564	−0.014	1.0×10^{-1}	119,804	0.052	**4.3×10^{-8}**	97,954	**3.9×10^{-8}**
rs7739232	HIPadjBMI	6	*KLHL31*	A	0.07	0.037	5.4×10^{-5}	131,877	0.063	**1.0×10^{-8}**	80,475	−0.004	7.5×10^{-1}	51,589	**2.9×10^{-5}**
rs13241538	HIPadjBMI	7	*KLF14*	C	0.48	0.017	1.6×10^{-6}	210,935	0.033	**9.9×10^{-14}**	117,210	−0.003	5.0×10^{-1}	93,911	**2.0×10^{-9}**
rs7044106	HIPadjBMI	9	*C5*	C	0.24	0.023	4.1×10^{-5}	143,412	0.039	**5.7×10^{-9}**	86,733	−0.003	6.9×10^{-1}	56,865	**1.3×10^{-5}**
rs11607976	HIP	11	*MYEOV*	C	0.70	0.022	**4.2×10^{-8}**	212,815	0.019	1.9×10^{-4}	118,391	0.024	7.7×10^{-6}	94,701	4.4×10^{-1}
rs1784203	WCadjBMI	11	*KIAA1731*	A	0.01	0.031	1.3×10^{-8}	63,892	0.000	9.9×10^{-1}	35,539	0.075	**1.0×10^{-19}**	28,353	1.2×10^{-1}
rs1394461	WHR	11	*CNTN5*	C	0.25	0.017	4.7×10^{-4}	144,349	0.035	**3.6×10^{-8}**	87,441	−0.011	1.6×10^{-1}	57,094	**1.1×10^{-6}**
rs319564	WHR	13	*GPC6*	C	0.45	0.014	3.4×10^{-5}	212,137	0.003	5.3E-01	117,970	0.027	**1.6×10^{-8}**	94,350	**6.0×10^{-5}**
rs2047937	WCadjBMI	16	*ZNF423*	C	0.50	0.019	**4.7×10^{-8}**	231,009	0.022	5.5×10^{-7}	127,288	0.014	3.6×10^{-3}	103,914	2.0×10^{-1}
rs2034088	HIPadjBMI	17	*VPS53*	T	0.53	0.021	4.8×10^{-9}	210,737	0.028	**9.6×10^{-10}**	117,142	0.014	6.5×10^{-3}	93,781	2.5×10^{-2}
rs1053593	HIPadjBMI	22	*HMGXB4*	T	0.65	0.021	3.9×10^{-8}	202,070	0.029	**1.8×10^{-9}**	114,347	0.011	5.1×10^{-2}	87,908	6.2×10^{-3}
Loci achieving genome-wide significance in all-ancestry meta-analyses															
rs1664789	WCadjBMI	5	*ARL15*	C	0.41	0.014	2.6×10^{-5}	244,110	0.005	2.8×10^{-1}	133,052	0.026	**3.6×10^{-8}**	109,025	**4.4×10^{-4}**
rs722585	HIPadjBMI	6	*GMDS*	G	0.68	0.015	2.1×10^{-4}	205,815	−0.001	8.8×10^{-1}	113,965	0.032	**9.2×10^{-9}**	89,831	**4.3×10^{-6}**
rs1144	WCadjBMI	7	*SRPK2*	C	0.34	0.019	**3.1×10^{-8}**	239,342	0.020	1.2×10^{-5}	131,398	0.018	4.1×10^{-4}	105,911	7.8×10^{-1}
rs2398893	WHR	9	*PTPDC1*	A	0.71	0.020	**4.0×10^{-8}**	226,572	0.019	5.1×10^{-5}	124,577	0.019	2.7×10^{-4}	99,968	9.5×10^{-1}
rs4985155‡	HIP	16	*PDXDC1*	A	0.66	0.018	4.5×10^{-7}	227,296	0.011	1.6×10^{-2}	125,048	0.029	**9.7×10^{-9}**	100,313	6.3×10^{-3}

P values and β coefficients for the association with the trait indicated in the meta-analysis of combined GWAS and Metabochip studies. The smallest *P* value for each SNP is shown in bold.
* The effect allele is the trait-increasing allele in the sex-combined analysis.
† Test for sex difference; values significant at the table-wise Bonferroni threshold of $0.05/19 = 2.63 \times 10^{-3}$ are marked in bold.
‡ $P = 7.3 \times 10^{-6}$ with height in ref. 43 (index SNP rs1136001; $r^2 = 0.79$, distance = 2,515 base pairs (bp)).

significantly larger effects ($P_{difference} < 0.05/19 = 0.003$) in one sex than in the other (Table 3, Supplementary Figs 1–4 and Supplementary Table 25). Three of four new loci with larger effects in women were associated with HIPadjBMI and three of five new loci with larger effects in men were associated with WCadjBMI. Most of the 19 loci showed some evidence of association with WHRadjBMI in sex-combined or sex-specific analyses, but four loci showed no association ($P > 0.01$) with WHRadjBMI, BMI, or height (Supplementary Tables 8 and 26).

We next asked whether the genes and pathways influencing these five traits are shared with WHRadjBMI or are distinct. Candidate genes were identified based on association with other traits, eQTLs, GRAIL and literature review (Extended Data Table 4 and Supplementary Tables 8, 11–13, 15–16 and 19). Candidate variants identified based on LD ($r^2 > 0.7$) included coding variants in *NTAN1* and *HMGXB4*, and six loci showed significant eQTLs in subcutaneous adipose tissue. On the basis of the literature, several candidate genes are involved in adipogenesis and insulin resistance. For example, delayed induction of preadipocyte transcription factor *ZNF423* in fibroblasts results in delayed adipogenesis[38], and *NLRP3* is part of inflammasome and pro-inflammatory T-cell populations in adipose tissue that contribute to inflammation and insulin resistance[39]. GRAIL analyses identified connections that partially overlap with those identified for WHRadjBMI (Supplementary Table 19). Taken together, the additional loci appear to function in processes similar to the WHRadjBMI loci. The identification of loci that are more strongly associated with WCadjBMI or HIPadjBMI than the other anthropometric traits suggests that the additional traits characterize aspects of central obesity and fat distribution that are not captured by WHRadjBMI or BMI alone.

Discussion

These meta-analyses of GWAS and Metabochip data in up to 224,459 individuals identified additional loci associated with waist and hip circumference measures and help to determine the role of common genetic variation in body fat distribution that is distinct from BMI and height. Our results emphasize the strong sexual dimorphism in the genetic regulation of fat distribution traits, a characteristic not observed for overall obesity as assessed by BMI[36]. Differences in body fat distribution between the sexes emerge in childhood, become more apparent during puberty[40], and change with menopause, generally attributed to the influence of sex hormones[41,42]. At loci with stronger effects in one sex than the other, these hormones may interact with transcription factors to regulate gene activity.

Annotation of the loci emphasized the role for mesenchymally derived tissues, especially adipose tissue, in fat distribution and central obesity. The development and regulation of adipose tissue deposition is closely associated with angiogenesis[29], a process highlighted by candidate genes at several WHRadjBMI loci. These tissues are implicated in insulin resistance, consistent with the enrichment of shared GWAS signals with lipids, T2D, and glycaemic traits. The identification of skeletal growth processes suggests that the underlying genes affect early development and/or differentiation of adipocytes from mesenchymal stem cells. By contrast, BMI has a substantial neuronal component, involving processes such as appetite regulation[36]. Our results provide a foundation for future biological research in the regulation of body fat distribution and its connections with cardiometabolic traits, and offer potential target mechanisms for interventions in the risks associated with abdominal fat accumulation.

Online Content Methods, along with any additional Extended Data display items and Source Data, are available in the online version of the paper; references unique to these sections appear only in the online paper.

Received 20 November 2013; accepted 2 December 2014.

1. Pischon, T. *et al.* General and abdominal adiposity and risk of death in Europe. *N. Engl. J. Med.* **359,** 2105–2120 (2008).
2. Wang, Y., Rimm, E. B., Stampfer, M. J., Willett, W. C. & Hu, F. B. Comparison of abdominal adiposity and overall obesity in predicting risk of type 2 diabetes among men. *Am. J. Clin. Nutr.* **81,** 555–563 (2005).
3. Canoy, D. Distribution of body fat and risk of coronary heart disease in men and women. *Curr. Opin. Cardiol.* **23,** 591–598 (2008).
4. Snijder, M. B. *et al.* Associations of hip and thigh circumferences independent of waist circumference with the incidence of type 2 diabetes: the Hoorn Study. *Am. J. Clin. Nutr.* **77,** 1192–1197 (2003).
5. Yusuf, S. *et al.* Obesity and the risk of myocardial infarction in 27,000 participants from 52 countries: a case-control study. *Lancet* **366,** 1640–1649 (2005).
6. Mason, C., Craig, C. L. & Katzmarzyk, P. T. Influence of central and extremity circumferences on all-cause mortality in men and women. *Obesity* **16,** 2690–2695 (2008).
7. Heid, I. M. *et al.* Meta-analysis identifies 13 new loci associated with waist-hip ratio and reveals sexual dimorphism in the genetic basis of fat distribution. *Nature Genet.* **42,** 949–960 (2010).
8. Randall, J. C. *et al.* Sex-stratified genome-wide association studies including 270,000 individuals show sexual dimorphism in genetic loci for anthropometric traits. *PLoS Genet.* **9,** e1003500 (2013).

9. Fox, C. S. *et al.* Genome-wide association of pericardial fat identifies a unique locus for ectopic fat. *PLoS Genet.* **8,** e1002705 (2012).
10. Fox, C. S. *et al.* Genome-wide association for abdominal subcutaneous and visceral adipose reveals a novel locus for visceral fat in women. *PLoS Genet.* **8,** e1002695 (2012).
11. Voight, B. F. *et al.* The metabochip, a custom genotyping array for genetic studies of metabolic, cardiovascular, and anthropometric traits. *PLoS Genet.* **8,** e1002793 (2012).
12. Sanna, S. *et al.* Common variants in the GDF5-UQCC region are associated with variation in human height. *Nature Genet.* **40,** 198–203 (2008).
13. Lango Allen, H. *et al.* Hundreds of variants clustered in genomic loci and biological pathways affect human height. *Nature* **467,** 832–838 (2010).
14. Yang, J. *et al.* Conditional and joint multiple-SNP analysis of GWAS summary statistics identifies additional variants influencing complex traits. *Nature Genet.* **44,** 369–375 (2012).
15. Yang, J. *et al.* Common SNPs explain a large proportion of the heritability for human height. *Nature Genet.* **42,** 565–569 (2010).
16. Hindorff, L. A. *et al.* A Catalog of Published Genome-Wide Association Studies. Available at http://www.genome.gov/gwastudies; accessed 31 January 2013.
17. Freathy, R. M. *et al.* Variants in *ADCY5* and near *CCNL1* are associated with fetal growth and birth weight. *Nature Genet.* **42,** 430–435 (2010).
18. Hoopes, S. L., Willcockson, H. H. & Caron, K. M. Characteristics of multi-organ lymphangiectasia resulting from temporal deletion of calcitonin receptor-like receptor in adult mice. *PLoS ONE* **7,** e45261 (2012).
19. Raychaudhuri, S. *et al.* Identifying relationships among genomic disease regions: predicting genes at pathogenic SNP associations and rare deletions. *PLoS Genet.* **5,** e1000534 (2009).
20. Segrè, A. V., Groop, L., Mootha, V. K., Daly, M. J. & Altshuler, D. Common inherited variation in mitochondrial genes is not enriched for associations with type 2 diabetes or related glycemic traits. *PLoS Genet.* **6,** e1001058 (2010).
21. Elias, I., Franckhauser, S. & Bosch, F. New insights into adipose tissue VEGF-A actions in the control of obesity and insulin resistance. *Adipocyte* **2,** 109–112 (2013).
22. Pal, A. *et al.* PTEN mutations as a cause of constitutive insulin sensitivity and obesity. *N. Engl. J. Med.* **367,** 1002–1011 (2012).
23. Pers, T. *et al.* Biological interpretation of genome-wide association studies using predicted gene functions. *Nature Commun.* **6,** 5890 (2015).
24. ENCODE Project Consortium. An integrated encyclopedia of DNA elements in the human genome. *Nature* **489,** 57–74 (2012).
25. Bernstein, B. E. *et al.* The NIH Roadmap Epigenomics Mapping Consortium. *Nature Biotechnol.* **28,** 1045–1048 (2010).
26. Nakagami, H. The mechanism of white and brown adipocyte differentiation. *Diabetes Metab. J.* **37,** 85–90 (2013).
27. Li, H. *et al.* miR-17–5p and miR-106a are involved in the balance between osteogenic and adipogenic differentiation of adipose-derived mesenchymal stem cells. *Stem Cell Res.* **10,** 313–324 (2013).
28. Mori, M., Nakagami, H., Rodriguez-Araujo, G., Nimura, K. & Kaneda, Y. Essential role for miR-196a in brown adipogenesis of white fat progenitor cells. *PLoS Biol.* **10,** e1001314 (2012).
29. Cao, Y. Angiogenesis and vascular functions in modulation of obesity, adipose metabolism, and insulin sensitivity. *Cell Metab.* **18,** 478–489 (2013).
30. Hagberg, C. E. *et al.* Vascular endothelial growth factor B controls endothelial fatty acid uptake. *Nature* **464,** 917–921 (2010).
31. Zygmunt, T. *et al.* Semaphorin-PlexinD1 signaling limits angiogenic potential via the VEGF decoy receptor sFlt1. *Dev. Cell* **21,** 301–314 (2011).
32. Shimizu, I. *et al.* Semaphorin3E-induced inflammation contributes to insulin resistance in dietary obesity. *Cell Metab.* **18,** 491–504 (2013).
33. Hanada, R. *et al.* Neuromedin U has a novel anorexigenic effect independent of the leptin signaling pathway. *Nature Med.* **10,** 1067–1073 (2004).
34. Huang, X. *et al.* FGFR4 prevents hyperlipidemia and insulin resistance but underlies high-fat diet induced fatty liver. *Diabetes* **56,** 2501–2510 (2007).
35. Foti, D. *et al.* Lack of the architectural factor HMGA1 causes insulin resistance and diabetes in humans and mice. *Nature Med.* **11,** 765–773 (2005).
36. Locke, A. E. *et al.* Genetic studies of body mass index yield new insights for obesity biology. *Nature* http://dx.doi.org/10.1038/nature14177 (this issue).
37. Wood, A. R. *et al.* Defining the role of common variation in the genomic and biological architecture of adult human height. *Nature Genet.* **46,** 1173–1186 (2014).
38. Jääger, K. & Neuman, T. Human dermal fibroblasts exhibit delayed adipogenic differentiation compared with mesenchymal stem cells. *Stem Cells Dev.* **20,** 1327–1336 (2011).
39. Goossens, G. H. *et al.* Expression of NLRP3 inflammasome and T cell population markers in adipose tissue are associated with insulin resistance and impaired glucose metabolism in humans. *Mol. Immunol.* **50,** 142–149 (2012).
40. Maynard, L. M. *et al.* Childhood body composition in relation to body mass index. *Pediatrics* **107,** 344–350 (2001).
41. Wells, J. C. Sexual dimorphism of body composition. *Best Pract. Res. Clin. Endocrinol. Metab.* **21,** 415–430 (2007).
42. Lovejoy, J. C., Champagne, C. M., de Jonge, L., Xie, H. & Smith, S. R. Increased visceral fat and decreased energy expenditure during the menopausal transition. *Int. J. Obes.* **32,** 949–958 (2008).
43. Okada, Y. *et al.* A genome-wide association study in 19,633 Japanese subjects identified LHX3-QSOX2 and IGF1 as adult height loci. *Hum. Mol. Genet.* **19,** 2303–2312 (2010).

Supplementary Information is available in the online version of the paper.

Acknowledgements We thank the more than 224,000 volunteers who participated in this study. Detailed acknowledgment of funding sources is provided in the Supplementary Note.

Author Contributions See the Supplementary Note for Author Contributions.

Author Information Summary results are available at http://www.broadinstitute.org/collaboration/giant/. Reprints and permissions information is available at www.nature.com/reprints. The authors declare competing financial interests: details are available in the online version of the paper. Readers are welcome to comment on the online version of the paper. Correspondence and requests for materials should be addressed to K.L.M. (mohlke@med.unc.edu) or C.M.L. (celi@well.ox.ac.uk).

Dmitry Shungin[1,2,3]*, Thomas W. Winkler[4]*, Damien C. Croteau-Chonka[5,6]*, Teresa Ferreira[7]*, Adam E. Locke[8]*, Reedik Mägi[7,9]*, Rona J. Strawbridge[10], Tune H. Pers[11,12,13,14], Krista Fischer[9], Anne E. Justice[15], Tsegaselassie Workalemahu[16], Joseph M. W. Wu[17], Martin L. Buchkovich[5], Nancy L. Heard-Costa[18,19], Tamara S. Roman[5], Alexander W. Drong[7], Ci Song[20,21,22], Stefan Gustafsson[21,22], Felix R. Day[23], Tonu Esko[9,11,12,13], Tove Fall[20,21,22], Zoltán Kutalik[24,25,26], Jian'an Luan[23], Joshua C. Randall[7,27], André Scherag[28,29], Sailaja Vedantam[11,12], Andrew R. Wood[30], Jin Chen[31], Rudolf Fehrmann[32], Juha Karjalainen[32], Bratati Kahali[33], Ching-Ti Liu[17], Ellen M. Schmidt[34], Devin Absher[35], Najaf Amin[36], Denise Anderson[37], Marian Beekman[38,39], Jennifer L. Bragg-Gresham[8,40], Steven Buyske[41,42], Ayse Demirkan[36,43], Georg B. Ehret[44,45], Mary F. Feitosa[46], Anuj Goel[7,47], Anne U. Jackson[8], Toby Johnson[25,26,48], Marcus E. Kleber[49,50], Kati Kristiansson[51], Massimo Mangino[52], Irene Mateo Leach[53], Carolina Medina-Gomez[54,55,56], Cameron D. Palmer[11,12], Dorota Pasko[30], Sonali Pechlivanis[28], Marjolein J. Peters[54,56], Inga Prokopenko[7,57,58], Alena Stančáková[59], Yun Ju Sung[60], Toshiko Tanaka[61], Alexander Teumer[62], Jana V. Van Vliet-Ostaptchouk[63], Loïc Yengo[64,65,66], Weihua Zhang[67,68], Eva Albrecht[69], Johan Ärnlöv[21,22,70], Gillian M. Arscott[71], Stefania Bandinelli[72], Amy Barrett[57], Claire Bellis[73,74], Amanda J. Bennett[57], Christian Berne[75], Matthias Blüher[76,77], Stefan Böhringer[38,78], Fabrice Bonnet[79], Yvonne Böttcher[76], Marcel Bruinenberg[80], Delia B. Carba[81], Ida H. Caspersen[82], Robert Clarke[83], E. Warwick Daw[46], Joris Deelen[38,39], Ewa Deelman[84], Graciela Delgado[49], Alex S. F. Doney[85], Niina Eklund[51,86], Michael R. Erdos[87], Karol Estrada[12,56,88], Elodie Eury[64,65,66], Nele Friedrich[89], Melissa E. Garcia[90], Vilmantas Giedraitis[91], Bruna Gigante[92], Alan S. Go[93], Alain Golay[94], Harald Grallert[69,95,96], Tanja B. Grammer[49], Jürgen Gräßler[97], Jagvir Grewal[67,68], Christopher J. Groves[57], Toomas Haller[9], Goran Hallmans[98], Catharina A. Hartman[99], Maija Hassinen[100], Caroline Hayward[101], Kauko Heikkilä[102], Karl-Heinz Herzig[103,104,105], Quinta Helmer[38,78,106], Hans L. Hillege[53,107], Oddgeir Holmen[108], Steven C. Hunt[109], Aaron Isaacs[36,110], Till Ittermann[111], Alan L. James[112,113], Ingegerd Johansson[3], Thorhildur Juliusdottir[7], Ioanna-Panagiota Kalafati[114], Leena Kinnunen[51], Wolfgang Koenig[50], Ishminder K. Kooner[67], Wolfgang Kratzer[115], Claudia Lamina[116], Karin Leander[92], Nanette R. Lee[81], Peter Lichtner[117], Lars Lind[118], Jaana Lindström[51], Stéphane Lobbens[64,65,66], Mattias Lorentzon[119], François Mach[45], Patrik K. E. Magnusson[20], Anubha Mahajan[7], Wendy L. McArdle[120], Cristina Menni[52], Sigrun Merger[121], Evelin Mihailov[9,122], Lili Milani[9], Rebecca Mills[67], Alireza Moayyeri[52,123], Keri L. Monda[15,124], Simon P. Mooijaart[38,125], Thomas W. Mühleisen[126,127], Antonella Mulas[128], Gabriele Müller[129], Martina Müller-Nurasyid[69,130,131,132], Ramaiah Nagaraja[133], Michael A. Nalls[134], Narisu Narisu[87], Nicola Glorioso[135], Ilja M. Nolte[107], Matthias Olden[4], Nigel W. Rayner[7,27,57], Frida Renstrom[2], Janina S. Ried[69], Neil R. Robertson[7,57], Lynda M. Rose[136], Serena Sanna[128], Hubert Scharnagl[137], Salome Scholtens[80], Bengt Sennblad[10,138], Thomas Seufferlein[115], Colleen M. Sitlani[139], Albert Vernon Smith[140,141], Kathleen Stirrups[27,142], Heather M. Stringham[8], Johan Sundström[118], Morris A. Swertz[32], Amy J. Swift[87], Ann-Christine Syvänen[21,143], Bamidele O. Tayo[144], Barbara Thorand[96,145], Gudmar Thorleifsson[146], Andreas Tomaschitz[147], Chiara Troffa[135], Floor V. A. van Oort[148], Niek Verweij[53], Judith M. Vonk[107], Lindsay L. Waite[35], Roman Wennauer[149], Tom Wilsgaard[150], Mary K. Wojczynski[46], Andrew Wong[151], Qunyuan Zhang[46], Jing Hua Zhao[23], Eoin P. Brennan[152], Murim Choi[153], Per Eriksson[10], Lasse Folkersen[10], Anders Franco-Cereceda[154], Ali G. Gharavi[155], Åsa K. Hedman[7,21,22], Marie-France Hivert[156,157], Jinyan Huang[158,159], Stavroula Kanoni[142], Fredrik Karpe[57,160], Sarah Keildson[7], Krzysztof Kiryluk[155], Liming Liang[159,161], Richard P. Lifton[162], Baoshan Ma[159,163], Amy J. McKnight[164], Ruth McPherson[165], Andres Metspalu[9,122], Josine L. Min[120], Miriam F. Moffatt[166], Grant W. Montgomery[167], Joanne M. Murabito[18,168], George Nicholson[169,170], Dale R. Nyholt[167,171], Christian Olsson[154], John R. B. Perry[7,30,52], Eva Reinmaa[9], Rany M. Salem[11,12,13], Niina Sandholm[172,173,174], Eric E. Schadt[175], Robert A. Scott[23], Lisette Stolk[38,56], Edgar E. Vallejo[176], Harm-Jan Westra[32], Krina T. Zondervan[7,177], The ADIPOGen Consortium†, The CARDIOGRAMplusC4D Consortium†, The CKDGen Consortium†, The GEFOS Consortium†, The GENIE Consortium†, The GLGC†, The ICBP†, The International Endogene Consortium†, The LifeLines Cohort Study†, The MAGIC Investigators†, The MuTHER Consortium†, The PAGE Consortium†, The ReproGen Consortium†, Philippe Amouyel[178], Dominique Arveiler[179], Stephan J. L. Bakker[180], John Beilby[71,181], Richard N. Bergman[182], John Blangero[73], Morris J. Brown[183], Michel Burnier[184], Harry Campbell[185], Aravinda Chakravarti[44], Peter S. Chines[87], Simone Claudi-Boehm[121], Francis S. Collins[87], Dana C. Crawford[186,187], John Danesh[188], Ulf de Faire[92], Eco J. C. de Geus[189,190], Marcus Dörr[191,192], Raimund Erbel[193], Johan G. Eriksson[51,194,195], Martin Farrall[7,47], Ele Ferrannini[196,197], Jean Ferrières[198], Nita G. Forouhi[23], Terrence Forrester[199], Oscar H. Franco[54,55], Ron T. Gansevoort[180], Christian Gieger[69], Vilmundur Gudnason[140,141], Christopher A. Haiman[200], Tamara B. Harris[90], Andrew T. Hattersley[201], Markku Heliövaara[51], Andrew A. Hicks[202], Aroon D. Hingorani[203], Wolfgang Hoffmann[111,192], Albert Hofman[54,55], Georg Homuth[62], Steve E. Humphries[204], Elina

Hyppönen[205,206,207,208], Thomas Illig[95,209], Marjo-Riitta Jarvelin[68,105,210,211,212,213], Berit Johansen[82], Pekka Jousilahti[51], Antti M. Jula[51], Jaakko Kaprio[51,86,102], Frank Kee[214], Sirkka M. Keinanen-Kiukaanniemi[215,216], Jaspal S. Kooner[67,166,217], Charles Kooperberg[218], Peter Kovacs[76,77], Aldi T. Kraja[46], Meena Kumari[219,220], Kari Kuulasmaa[51], Johanna Kuusisto[221], Timo A. Lakka[100,222,223], Claudia Langenberg[23,219], Loic Le Marchand[224], Terho Lehtimäki[225], Valeriya Lyssenko[226,227], Satu Männistö[51], André Marette[228,229], Tara C. Matise[42], Colin A. McKenzie[199], Barbara McKnight[230], Arthur W. Musk[231], Stefan Möhlenkamp[193], Andrew D. Morris[85], Mari Nelis[9], Claes Ohlsson[119], Albertine J. Oldehinkel[99], Ken K. Ong[23,151], Lyle J. Palmer[232,233], Brenda W. Penninx[190,234], Annette Peters[95,132,145], Peter P. Pramstaller[202,235], Olli T. Raitakari[236,237], Tuomo Rankinen[238], D. C. Rao[46,60,239], Treva K. Rice[60,239], Paul M. Ridker[136,240], Marylyn D. Ritchie[241], Igor Rudan[185,242], Veikko Salomaa[51], Nilesh J. Samani[243,244], Jouko Saramies[245], Mark A. Sarzynski[238], Peter E. H. Schwarz[97,246], Alan R. Shuldiner[247,248,249], Jan A. Staessen[250,251], Valgerdur Steinthorsdottir[146], Ronald P. Stolk[107], Konstantin Strauch[69,131], Anke Tönjes[76,77], Angelo Tremblay[252], Elena Tremoli[253], Marie-Claude Vohl[229,254], Uwe Völker[62,192], Peter Vollenweider[255], James F. Wilson[185], Jacqueline C. Witteman[55], Linda S. Adair[256], Murielle Bochud[257,258], Bernhard O. Boehm[259,260], Stefan R. Bornstein[97], Claude Bouchard[238], Stéphane Cauchi[64,65,66], Mark J. Caulfield[261], John C. Chambers[67,68,217], Daniel I. Chasman[136,240], Richard S. Cooper[144], George Dedoussis[114], Luigi Ferrucci[61], Philippe Froguel[58,64,65,66], Hans-Jörgen Grabe[262,263], Anders Hamsten[10], Jennie Hui[71,181,264], Kristian Hveem[108], Karl-Heinz Jöckel[28], Mika Kivimaki[219], Diana Kuh[151], Markku Laakso[221], Yongmei Liu[265], Winfried März[49,137,266], Patricia B. Munroe[261], Inger Njølstad[150], Ben A. Oostra[36,110,267], Colin N. A. Palmer[85], Nancy L. Pedersen[20], Markus Perola[9,51,86], Louis Pérusse[229,252], Ulrike Peters[218], Chris Power[208], Thomas Quertermous[268], Rainer Rauramaa[100,223], Fernando Rivadeneira[54,55,56], Timo E. Saaristo[269,270], Danish Saleheen[188,271,272], Juha Sinisalo[273], P. Eline Slagboom[38,39], Harold Snieder[107], Tim D. Spector[52], Unnur Thorsteinsdottir[146,274], Michael Stumvoll[76,77], Jaakko Tuomilehto[51,275,276,277], André G. Uitterlinden[54,55,56], Matti Uusitupa[278,279], Pim van der Harst[32,53,280], Giovanni Veronesi[281], Mark Walker[282], Nicholas J. Wareham[23], Hugh Watkins[7,47], H-Erich Wichmann[283,284,285], Goncalo R. Abecasis[8], Themistocles L. Assimes[268], Sonja I. Berndt[286], Michael Boehnke[8], Ingrid B. Borecki[46], Panos Deloukas[27,142,287], Lude Franke[32], Timothy M. Frayling[30], Leif C. Groop[86,227], David J. Hunter[6,16,159], Robert C. Kaplan[288], Jeffrey R. O'Connell[247,248], Lu Qi[6,16], David Schlessinger[133], David P. Strachan[289], Kari Stefansson[146,274], Cornelia M. van Duijn[36,54,55,110], Cristen J. Willer[31,34,290], Peter M. Visscher[291,292], Jian Yang[291,292], Joel N. Hirschhorn[11,12,13], M. Carola Zillikens[54,56], Mark I. McCarthy[7,57,293], Elizabeth K. Speliotes[33], Kari E. North[15,294], Caroline S. Fox[18], Inês Barroso[27,295,296], Paul W. Franks[1,2,16], Erik Ingelsson[7,21,22], Iris M. Heid[4,69]§, Ruth J. F. Loos[23,297,298,299]§, L. Adrienne Cupples[17,18]§, Andrew P. Morris[7,9,300]§, Cecilia M. Lindgren[7,12]§ & Karen L Mohlke[5]§

[1]Department of Public Health and Clinical Medicine, Unit of Medicine, Umeå University, 901 87 Umeå, Sweden. [2]Department of Clinical Sciences, Genetic & Molecular Epidemiology Unit, Lund University Diabetes Center, Skåne University Hosptial, 205 02 Malmö, Sweden. [3]Department of Odontology, Umeå University, 901 85 Umeå, Sweden. [4]Department of Genetic Epidemiology, Institute of Epidemiology and Preventive Medicine, University of Regensburg, D-93053 Regensburg, Germany. [5]Department of Genetics, University of North Carolina, Chapel Hill, North Carolina 27599, USA. [6]Channing Division of Network Medicine, Department of Medicine, Brigham and Women's Hospital and Harvard Medical School, Boston, Massachusetts 02115, USA. [7]Wellcome Trust Centre for Human Genetics, University of Oxford, Oxford OX3 7BN, UK. [8]Center for Statistical Genetics, Department of Biostatistics, University of Michigan, Ann Arbor, Michigan 48109, USA. [9]Estonian Genome Center, University of Tartu, Tartu 51010, Estonia. [10]Atherosclerosis Research Unit, Center for Molecular Medicine, Department of Medicine, Karolinska Institutet, Stockholm 17176, Sweden. [11]Divisions of Endocrinology and Genetics and Center for Basic and Translational Obesity Research, Boston Children's Hospital, Boston, Massachusetts 02115, USA. [12]Broad Institute of the Massachusetts Institute of Technology and Harvard University, Cambridge, Massachusetts 02142, USA. [13]Department of Genetics, Harvard Medical School, Boston, Massachusetts 02115, USA. [14]Center for Biological Sequence Analysis, Department of Systems Biology, Technical University of Denmark, Lyngby 2800, Denmark. [15]Department of Epidemiology, University of North Carolina at Chapel Hill, Chapel Hill, North Carolina 27599, USA. [16]Department of Nutrition, Harvard School of Public Health, Boston, Massachusetts 02115, USA. [17]Department of Biostatistics, Boston University School of Public Health, Boston, Massachusetts 02118, USA. [18]National Heart, Lung, and Blood Institute, the Framingham Heart Study, Framingham Massachusetts 01702, USA. [19]Department of Neurology, Boston University School of Medicine, Boston, Massachusetts 02118, USA. [20]Department of Medical Epidemiology and Biostatistics, Karolinska Institutet, Stockholm 17177, Sweden. [21]Science for Life Laboratory, Uppsala University, Uppsala 75185, Sweden. [22]Department of Medical Sciences, Molecular Epidemiology, Uppsala University, Uppsala 75185, Sweden. [23]MRC Epidemiology Unit, University of Cambridge School of Clinical Medicine, Institute of Metabolic Science, Cambridge Biomedical Campus, Cambridge CB2 0QQ, UK. [24]Institute of Social and Preventive Medicine (IUMSP), Centre Hospitalier Universitaire Vaudois (CHUV), Lausanne 1010, Switzerland. [25]Swiss Institute of Bioinformatics, Lausanne 1015, Switzerland. [26]Department of Medical Genetics, University of Lausanne, Lausanne 1005, Switzerland. [27]Wellcome Trust Sanger Institute, Hinxton, Cambridge CB10 1SA, UK. [28]Institute for Medical Informatics, Biometry and Epidemiology (IMIBE), University Hospital Essen, Essen, 45147 Germany. [29]Clinical Epidemiology, Integrated Research and Treatment Center, Center for Sepsis Control and Care (CSCC), Jena University Hospital, Jena 07743, Germany. [30]Genetics of Complex Traits, University of Exeter Medical School, University of Exeter, Exeter EX1 2LU, UK. [31]Department of Internal Medicine, Division of Cardiovascular Medicine, University of Michigan, Ann Arbor, Michigan 48109, USA. [32]Department of Genetics, University Medical Center Groningen, University of Groningen, 9700 RB Groningen, The Netherlands. [33]Department of Internal Medicine, Division of Gastroenterology, and Department of Computational Medicine and Bioinformatics, University of Michigan, Ann Arbor, Michigan 48109, USA. [34]Department of Computational Medicine and Bioinformatics, University of Michigan, Ann Arbor, Michigan 48109, USA. [35]HudsonAlpha Institute for Biotechnology, Huntsville, Alabama 35806, USA. [36]Genetic Epidemiology Unit, Department of Epidemiology, Erasmus MC University Medical Center, 3015 GE Rotterdam, The Netherlands. [37]Telethon Institute for Child Health Research, Centre for Child Health Research, The University of Western Australia, Perth, Western Australia 6008, Australia. [38]Netherlands Consortium for Healthy Aging (NCHA), Leiden University Medical Center, Leiden 2300 RC, The Netherlands. [39]Department of Molecular Epidemiology, Leiden University Medical Center, 2300 RC Leiden, The Netherlands. [40]Kidney Epidemiology and Cost Center, University of Michigan, Ann Arbor, Michigan 48109, USA. [41]Department of Statistics & Biostatistics, Rutgers University, Piscataway, New Jersey 08854, USA. [42]Department of Genetics, Rutgers University, Piscataway, New Jersey 08854, USA. [43]Department of Human Genetics, Leiden University Medical Center, 2333 ZC Leiden, The Netherlands. [44]Center for Complex Disease Genomics, McKusick-Nathans Institute of Genetic Medicine, Johns Hopkins University School of Medicine, Baltimore, Maryland 21205, USA. [45]Cardiology, Department of Specialties of Internal Medicine, Geneva University Hospital, Geneva 1211, Switzerland. [46]Department of Genetics, Washington University School of Medicine, St Louis, Missouri 63110, USA. [47]Division of Cardiovascular Medicine, Radcliffe Department of Medicine, University of Oxford, Oxford OX3 9DU, UK. [48]University Institute for Social and Preventative Medicine, Centre Hospitalier Universitaire Vaudois (CHUV), University of Lausanne, Lausanne 1005, Switzerland. [49]Vth Department of Medicine (Nephrology, Hypertensiology, Endocrinology, Diabetology, Rheumatology), Medical Faculty of Mannheim, University of Heidelberg, D-68187 Mannheim, Germany. [50]Department of Internal Medicine II, Ulm University Medical Centre, D-89081 Ulm, Germany. [51]National Institute for Health and Welfare, FI-00271 Helsinki, Finland. [52]Department of Twin Research and Genetic Epidemiology, King's College London, London SE1 7EH, UK. [53]Department of Cardiology, University Medical Center Groningen, University of Groningen, 9700RB Groningen, The Netherlands. [54]Netherlands Consortium for Healthy Aging (NCHA), 3015GE Rotterdam, The Netherlands. [55]Department of Epidemiology, Erasmus MC University Medical Center, 3015GE Rotterdam, The Netherlands. [56]Department of Internal Medicine, Erasmus MC University Medical Center, 3015GE Rotterdam, The Netherlands. [57]Oxford Centre for Diabetes, Endocrinology and Metabolism, University of Oxford, Oxford OX3 7LJ, UK. [58]Department of Genomics of Common Disease, School of Public Health, Imperial College London, Hammersmith Hospital, London W12 0NN, UK. [59]University of Eastern Finland, FI-70210 Kuopio, Finland. [60]Division of Biostatistics, Washington University School of Medicine, St Louis, Missouri 63110, USA. [61]Translational Gerontology Branch, National Institute on Aging, Baltimore, Maryland 21225, USA. [62]Interfaculty Institute for Genetics and Functional Genomics, University Medicine Greifswald, D-17475 Greifswald, Germany. [63]Department of Endocrinology, University of Groningen, University Medical Center Groningen, Groningen, 9700 RB, The Netherlands. [64]CNRS UMR 8199, F-59019 Lille, France. [65]European Genomic Institute for Diabetes, F-59000 Lille, France. [66]Université de Lille 2, F-59000 Lille, France. [67]Ealing Hospital NHS Trust, Middlesex UB1 3HW, UK. [68]Department of Epidemiology and Biostatistics, Imperial College London, London W2 1PG, UK. [69]Institute of Genetic Epidemiology, Helmholtz Zentrum München - German Research Center for Environmental Health, D-85764 Neuherberg, Germany. [70]School of Health and Social Studies, Dalarna University, SE-791 88 Falun, Sweden. [71]PathWest Laboratory Medicine of Western Australia, Nedlands, Western Australia 6009, Australia. [72]Geriatric Unit, Azienda Sanitaria Firenze (ASF), 50125 Florence, Italy. [73]Department of Genetics, Texas Biomedical Research Institute, San Antonio, Texas 78227, USA. [74]Genomics Research Centre, Institute of Health and Biomedical Innovation, Queensland University of Technology, Brisbane, Queensland 4001, Australia. [75]Department of Medical Sciences, Endocrinology, Diabetes and Metabolism, Uppsala University, Uppsala 75185, Sweden. [76]Integrated Research and Treatment Center (IFB) Adiposity Diseases, University of Leipzig, D-04103 Leipzig, Germany. [77]Department of Medicine, University of Leipzig, D-04103 Leipzig, Germany. [78]Department of Medical Statistics and Bioinformatics, Leiden University Medical Center, 2300 RC Leiden, The Netherlands. [79]Inserm UMR991, Department of Endocrinology, University of Rennes, F-35000 Rennes, France. [80]LifeLines Cohort Study, University Medical Center Groningen, University of Groningen, 9700 RB Groningen, The Netherlands. [81]USC-Office of Population Studies Foundation, Inc., University of San Carlos, Cebu City 6000, Philippines. [82]Department of Biology, Norwegian University of Science and Technology, 7491 Trondheim, Norway. [83]Clinical Trial Service Unit and Epidemiological Studies Unit, Nuffield Department of Population Health, University of Oxford, Oxford OX3 7LF, UK. [84]Information Sciences Institute, University of Southern California, Marina del Rey, California 90292, USA. [85]Medical Research Institute, University of Dundee, Ninewells Hospital and Medical School, Dundee DD1 9SY, UK. [86]Institute for Molecular Medicine, University of Helsinki, FI-00014 Helsinki, Finland. [87]Medical Genomics and Metabolic Genetics Branch, National Human Genome Research Institute, NIH, Bethesda, Maryland 20892, USA. [88]Analytic and Translational Genetics Unit, Massachusetts General Hospital and Harvard Medical School, Boston, Massachusetts 02114, USA. [89]Institute of Clinical Chemistry and Laboratory Medicine, University Medicine Greifswald, D-17475 Greifswald, Germany. [90]Laboratory of Epidemiology and Population Sciences, National Institute on Aging, NIH, Bethesda, Maryland 20892, USA. [91]Department of Public Health and Caring Sciences, Geriatrics, Uppsala University, Uppsala 75185, Sweden. [92]Division of Cardiovascular Epidemiology, Institute of Environmental Medicine, Karolinska Institutet, Stockholm, Sweden, Stockholm 17177, Sweden. [93]Kaiser Permanente, Division of Research, Oakland, California 94612, USA. [94]Service of Therapeutic Education for Diabetes, Obesity and Chronic Diseases, Geneva University Hospital, Geneva CH-1211, Switzerland. [95]Research Unit of Molecular Epidemiology, Helmholtz Zentrum München - German Research Center for Environmental Health, D-85764 Neuherberg, Germany. [96]German Center for Diabetes Research (DZD), D-85764 Neuherberg, Germany. [97]Department of Medicine III, University Hospital Carl Gustav Carus, Technische Universität Dresden, D-01307 Dresden, Germany. [98]Department of Public Health and Clinical Medicine, Unit of Nutritional Research, Umeå University, Umeå 90187, Sweden. [99]Department of Psychiatry, University of Groningen, University Medical Center

Groningen, 9700RB Groningen, The Netherlands. [100]Kuopio Research Institute of Exercise Medicine, FI-70100 Kuopio, Finland. [101]MRC Human Genetics Unit, Institute of Genetics and Molecular Medicine, University of Edinburgh, Western General Hospital, Edinburgh EH4 2XU, UK. [102]Hjelt Institute Department of Public Health, University of Helsinki, FI-00014 Helsinki, Finland. [103]Institute of Biomedicine, University of Oulu, FI-90014 Oulu, Finland. [104]Medical Research Center Oulu and Oulu University Hospital, FI-90014 Oulu, Finland. [105]Biocenter Oulu, University of Oulu, FI-90014 Oulu, Finland. [106]Faculty of Psychology and Education, VU University Amsterdam, 1081BT Amsterdam, The Netherlands. [107]Department of Epidemiology, University Medical Center Groningen, University of Groningen, 9700 RB Groningen, The Netherlands. [108]Department of Public Health and General Practice, Norwegian University of Science and Technology, Trondheim 7489, Norway. [109]Cardiovascular Genetics Division, Department of Internal Medicine, University of Utah, Salt Lake City, Utah 84108, USA. [110]Center for Medical Sytems Biology, 2300 RC Leiden, The Netherlands. [111]Institute for Community Medicine, University Medicine Greifswald, D-17475 Greifswald, Germany. [112]Department of Pulmonary Physiology and Sleep Medicine, Nedlands, Western Australia 6009, Australia. [113]School of Medicine and Pharmacology, University of Western Australia, Crawley 6009, Australia. [114]Department of Dietetics-Nutrition, Harokopio University, 17671 Athens, Greece. [115]Department of Internal Medicine I, Ulm University Medical Centre, D-89081 Ulm, Germany. [116]Division of Genetic Epidemiology, Department of Medical Genetics, Molecular and Clinical Pharmacology, Innsbruck Medical University, 6020 Innsbruck, Austria. [117]Institute of Human Genetics, Helmholtz Zentrum München - German Research Center for Environmental Health, D-85764 Neuherberg, Germany. [118]Department of Medical Sciences, Cardiovascular Epidemiology, Uppsala University, Uppsala 75185, Sweden. [119]Centre for Bone and Arthritis Research, Department of Internal Medicine and Clinical Nutrition, Institute of Medicine, Sahlgrenska Academy, University of Gothenburg, Gothenburg 413 45, Sweden. [120]School of Social and Community Medicine, University of Bristol, Bristol BS8 2BN, UK. [121]Division of Endocrinology, Diabetes and Metabolism, Ulm University Medical Centre, D-89081 Ulm, Germany. [122]Institute of Molecular and Cell Biology, University of Tartu, Tartu 51010, Estonia. [123]Farr Institute of Health Informatics Research, University College London, London NW1 2DA, UK [124]The Center for Observational Research, Amgen, Inc., Thousand Oaks, California 91320, USA. [125]Department of Gerontology and Geriatrics, Leiden University Medical Center, 2300 RC Leiden, The Netherlands. [126]Department of Genomics, Life & Brain Center, University of Bonn, 53127 Bonn, Germany. [127]Institute of Human Genetics, University of Bonn, 53127 Bonn, Germany. [128]Istituto di Ricerca Genetica e Biomedica (IRGB), Consiglio Nazionale delle Ricerche, Cagliari, Sardinia 09042, Italy. [129]Center for Evidence-based Healthcare, University Hospital Carl Gustav Carus, Technische Universität Dresden, D-01307 Dresden, Germany. [130]Department of Medicine I, University Hospital Grosshadern, Ludwig-Maximilians-Universität, D-81377 Munich, Germany. [131]Institute of Medical Informatics, Biometry and Epidemiology, Chair of Genetic Epidemiology, Ludwig-Maximilians-Universität, D-81377 Munich, Germany. [132]Deutsches Forschungszentrum für Herz-Kreislauferkrankungen (DZHK) (German Research Centre for Cardiovascular Research), Munich Heart Alliance, D-80636 Munich, Germany. [133]Laboratory of Genetics, National Institute on Aging, Baltimore, Maryland 21224, USA. [134]Laboratory of Neurogenetics, National Institute on Aging, National Institutes of Health, Bethesda, Maryland 20892, USA. [135]Hypertension and Related Diseases Centre - AOU, University of Sassari Medical School, Sassari 07100, Italy. [136]Division of Preventive Medicine, Brigham and Women's Hospital, Boston, Massachusetts 02215, USA. [137]Clinical Institute of Medical and Chemical Laboratory Diagnostics, Medical University of Graz, Graz 8036, Austria. [138]Science for Life Laboratory, Karolinska Institutet, Stockholm 171 65, Sweden. [139]Department of Medicine, University of Washington, Seattle, Washington 98101, USA. [140]Icelandic Heart Association, Kopavogur 201, Iceland. [141]University of Iceland, Reykjavik 101, Iceland. [142]William Harvey Research Institute, Barts and The London School of Medicine and Dentistry, Queen Mary University of London, London EC1M 6BQ, UK. [143]Department of Medical Sciences, Molecular Medicine, Uppsala University, Uppsala 75144, Sweden. [144]Department of Public Health Sciences, Stritch School of Medicine, Loyola University of Chicago, Maywood, Illinois 61053, USA. [145]Institute of Epidemiology II, Helmholtz Zentrum München - German Research Center for Environmental Health, Neuherberg, Germany, D-85764 Neuherberg, Germany. [146]deCODE Genetics, Amgen Inc., Reykjavik 101, Iceland. [147]Department of Cardiology, Medical University of Graz, Graz 8036, Austria. [148]Department of Child and Adolescent Psychiatry, Psychology, Erasmus MC University Medical Centre, 3000 CB Rotterdam, The Netherlands. [149]Department of Clinical Chemistry, Ulm University Medical Centre, D-89081 Ulm, Germany. [150]Department of Community Medicine, Faculty of Health Sciences, UiT The Arctic University of Norway, 9037 Tromsø, Norway. [151]MRC Unit for Lifelong Health and Ageing at University College London, London WC1B 5JU, UK. [152]Diabetes Complications Research Centre, Conway Institute, School of Medicine and Medical Sciences, University College Dublin, Dublin 4, Ireland. [153]Department of Biomedical Sciences, Seoul National University College of Medicine, Seoul 110-799, Korea. [154]Cardiothoracic Surgery Unit, Department of Molecular Medicine and Surgery, Karolinska Institutet, Stockholm 17176, Sweden. [155]Department of Medicine, Columbia University College of Physicians and Surgeons, New York 10032, USA. [156]Department of Population Medicine, Harvard Pilgrim Health Care Institute, Harvard Medical School, Boston, Massachusetts 02215, USA. [157]Massachusetts General Hospital, Boston, Massachusetts 02114, USA. [158]State Key Laboratory of Medical Genomics, Shanghai Institute of Hematology, Rui Jin Hospital Affiliated with Shanghai Jiao Tong University School of Medicine, Shanghai 200025, China. [159]Department of Epidemiology, Harvard School of Public Health, Boston, Massachusetts 02115, USA. [160]NIHR Oxford Biomedical Research Centre, OUH Trust, Oxford OX3 7LE, UK. [161]Harvard School of Public Health, Department of Biostatistics, Harvard University, Boston, Massachusetts 02115, USA. [162]Department of Genetics, Howard Hughes Medical Institute, Yale University School of Medicine, New Haven, New Haven, Connecticut 06520, USA. [163]College of Information Science and Technology, Dalian Maritime University, Dalian, Liaoning 116026, China. [164]Nephrology Research, Centre for Public Health, Queen's University of Belfast, Belfast, County Down BT9 7AB, UK. [165]University of Ottawa Heart Institute, Ottawa K1Y 4W7, Canada. [166]National Heart and Lung Institute, Imperial College London, London SW3 6LY, UK. [167]QIMR Berghofer Medical Research Institute, Brisbane, Queensland 4006, Australia. [168]Section of General Internal Medicine, Boston University School of Medicine, Boston, Massachusetts 02118, USA. [169]Department of Statistics, University of Oxford, 1 South Parks Road, Oxford OX1 3TG, UK. [170]MRC Harwell, Harwell Science and Innovation Campus, Harwell OX11 0QG, UK. [171]Institute of Health and Biomedical Innovation, Queensland University of Technology, Brisbane, Queensland 4059, Australia. [172]Department of Biomedical Engineering and Computational Science, Aalto University School of Science, FI-00076 Helsinki, Finland. [173]Department of Medicine, Division of Nephrology, Helsinki University Central Hospital, FI-00290 Helsinki, Finland. [174]Folkhälsan Institute of Genetics, Folkhälsan Research Center, FI-00290 Helsinki, Finland. [175]Icahn Institute for Genomics and Multiscale Biology, Icahn School of Medicine at Mount Sinai, New York, New York 10580, USA. [176]Computer Science Department, Tecnológico de Monterrey, Atizapán de Zaragoza, 52926, Mexico. [177]Nuffield Department of Obstetrics & Gynaecology, University of Oxford, Oxford OX3 7BN, UK. [178]Institut Pasteur de Lille; INSERM, U744; Université de Lille 2; F-59000 Lille, France. [179]Department of Epidemiology and Public Health, EA3430, University of Strasbourg, Faculty of Medicine, Strasbourg, France. [180]Department of Internal Medicine, University Medical Center Groningen, University of Groningen, 9700RB Groningen, The Netherlands. [181]Pathology and Laboratory Medicine, The University of Western Australia, Perth, Western Australia 6009, Australia. [182]Cedars-Sinai Diabetes and Obesity Research Institute, Los Angeles, California 90048, USA. [183]Clinical Pharmacology Unit, University of Cambridge, Addenbrooke's Hospital, Hills Road, Cambridge CB2 2QQ, UK. [184]Service of Nephrology, Department of Medicine, Lausanne University Hospital (CHUV), Lausanne 1005, Switzerland. [185]Centre for Population Health Sciences, University of Edinburgh, Teviot Place, Edinburgh EH8 9AG, UK. [186]Center for Human Genetics Research, Vanderbilt University Medical Center, Nashville, Tennessee 37203, USA. [187]Department of Molecular Physiology and Biophysics, Vanderbilt University, Nashville, Tennessee 37232, USA. [188]Department of Public Health and Primary Care, University of Cambridge, Cambridge CB1 8RN, UK. [189]Biological Psychology, VU University Amsterdam, 1081BT Amsterdam, The Netherlands. [190]Institute for Research in Extramural Medicine, Institute for Health and Care Research, VU University, 1081BT Amsterdam, The Netherlands. [191]Department of Internal Medicine B, University Medicine Greifswald, D-17475 Greifswald, Germany. [192]DZHK (Deutsches Zentrum für Herz-Kreislaufforschung – German Centre for Cardiovascular Research), partner site Greifswald, D-17475 Greifswald, Germany. [193]Clinic of Cardiology, West-German Heart Centre, University Hospital Essen, 45122 Essen, Germany. [194]Department of General Practice and Primary Health Care, University of Helsinki, FI-00290 Helsinki, Finland. [195]Unit of General Practice, Helsinki University Central Hospital, Helsinki FI-00290, Finland. [196]Department of Internal Medicine, University of Pisa, Pisa 56100, Italy. [197]National Research Council Institute of Clinical Physiology, University of Pisa, Pisa 56124, Italy. [198]Department of Cardiology, Toulouse University School of Medicine, Rangueil Hospital, 31400 Toulouse, France. [199]UWI Solutions for Developing Countries, The University of the West Indies, Mona, Kingston 7, Jamaica. [200]Department of Preventive Medicine, Keck School of Medicine, University of Southern California, Los Angeles, California 90089, USA. [201]Institute of Biomedical & Clinical Science, University of Exeter, Barrack Road, Exeter EX2 5DW, UK. [202]Center for Biomedicine, European Academy Bozen, Bolzano (EURAC), Bolzano 39100, Italy (affiliated Institute of the University of Lübeck, D-23562 Lübeck, Germany). [203]Institute of Cardiovascular Science, University College London, London WC1E 6BT, UK. [204]Centre for Cardiovascular Genetics, Institute Cardiovascular Sciences, University College London, London WC1E 6JJ, UK. [205]Sansom Institute for Health Research, University of South Australia, Adelaide 5000, South Australia, Australia. [206]School of Population Health, University of South Australia, Adelaide 5000, South Australia, Australia. [207]South Australian Health and Medical Research Institute, Adelaide 5000, South Australia, Australia. [208]Population, Policy, and Practice, University College London Institute of Child Health, London WC1N 1EH, UK. [209]Hannover Unified Biobank, Hannover Medical School, Hannover, D-30625 Hannover, Germany. [210]National Institute for Health and Welfare, FI-90101 Oulu, Finland. [211]MRC Health Protection Agency (HPA) Centre for Environment and Health, School of Public Health, Imperial College London, London W2 1PG, UK. [212]Unit of Primary Care, Oulu University Hospital, FI-90220 Oulu, Finland. [213]Institute of Health Sciences, University of Oulu, FI-90014 Oulu, Finland. [214]UK Clinical Research Collaboration Centre of Excellence for Public Health (NI), Queens University of Belfast, Belfast BT7 1NN, Northern Ireland, UK. [215]Institute of Health Sciences, Faculty of Medicine, University of Oulu, FI-90014 Oulu, Finland. [216]Unit of Primary Health Care/ General Practice, Oulu University Hospital, FI-90220 Oulu, Finland. [217]Imperial College Healthcare NHS Trust, London W12 0HS, UK. [218]Division of Public Health Sciences, Fred Hutchinson Cancer Research Center, Seattle, Washington 98109, USA. [219]Department of Epidemiology and Public Health, University College London, London WC1E 6BT, UK. [220]Department of Biological and Social Epidemiology, University of Essex, Wivenhoe Park, Colchester, Essex CO4 3SQ, UK. [221]Department of Medicine, Kuopio University Hospital and University of Eastern Finland, FI-70210 Kuopio, Finland. [222]Department of Physiology, Institute of Biomedicine, University of Eastern Finland, Kuopio Campus, FI-70211 Kuopio, Finland. [223]Department of Clinical Physiology and Nuclear Medicine, Kuopio University Hospital and University of Eastern Finland, FI-70210 Kuopio, Finland. [224]Epidemiology Program, University of Hawaii Cancer Center, Honolulu, Hawaii 96813, USA. [225]Department of Clinical Chemistry, Fimlab Laboratories and School of Medicine University of Tampere, FI-33520 Tampere, Finland. [226]Steno Diabetes Center A/S, Gentofte DK-2820, Denmark. [227]Lund University Diabetes Centre and Department of Clinical Science, Diabetes & Endocrinology Unit, Lund University, Malmö 221 00, Sweden. [228]Institut Universitaire de Cardiologie et de Pneumologie de Québec, Faculty of Medicine, Laval University, Quebec QC G1V 0A6, Canada. [229]Institute of Nutrition and Functional Foods, Laval University, Quebec QC G1V 0A6, Canada. [230]Department of Biostatistics, University of Washington, Seattle, Washington 98195, USA. [231]Department of Respiratory Medicine, Sir Charles Gairdner Hospital, Nedlands, Western Australia 6009, Australia. [232]Epidemiology and Obstetrics & Gynaecology, University of Toronto, Toronto, Ontario M5G 1E2, Canada. [233]Genetic Epidemiology & Biostatistics Platform, Ontario Institute for Cancer Research, Toronto, Ontario M5G 0A3, Canada. [234]Department

of Psychiatry, Neuroscience Campus, VU University Amsterdam, 1081 BT Amsterdam, The Netherlands. [235]Department of Neurology, General Central Hospital, Bolzano 39100, Italy. [236]Department of Clinical Physiology and Nuclear Medicine, Turku University Hospital, FI-20521 Turku, Finland. [237]Research Centre of Applied and Preventive Cardiovascular Medicine, University of Turku, FI-20521 Turku, Finland. [238]Human Genomics Laboratory, Pennington Biomedical Research Center, Baton Rouge, Louisiana 70808, USA. [239]Department of Psychiatry, Washington University School of Medicine, St Louis, Missouri 63110, USA. [240]Harvard Medical School, Boston, Massachusetts 02115, USA. [241]Center for Systems Genomics, The Pennsylvania State University, University Park, Pennsylvania 16802, USA. [242]Croatian Centre for Global Health, Faculty of Medicine, University of Split, 21000 Split, Croatia. [243]Department of Cardiovascular Sciences, University of Leicester, Glenfield Hospital, Leicester LE3 9QP, UK. [244]National Institute for Health Research (NIHR) Leicester Cardiovascular Biomedical Research Unit, Glenfield Hospital, Leicester LE3 9QP, UK. [245]South Carelia Central Hospital, 53130 Lappeenranta, Finland. [246]Paul Langerhans Institute Dresden, German Center for Diabetes Research (DZD), 01307 Dresden, Germany. [247]Division of Endocrinology, Diabetes and Nutrition, University of Maryland School of Medicine, Baltimore, Maryland 21201, USA. [248]Program for Personalized and Genomic Medicine, University of Maryland School of Medicine, Baltimore, Maryland 21201, USA. [249]Geriatric Research and Education Clinical Center, Veterans Administration Medical Center, Baltimore, Maryland 21201, USA. [250]Department of Epidemiology, Maastricht University, 6229 HA Maastricht, The Netherlands. [251]Research Unit Hypertension and Cardiovascular Epidemiology, KU Leuven Department of Cardiovascular Sciences, University of Leuven, B-3000 Leuven, Belgium. [252]Department of Kinesiology, Laval University, Quebec, QC G1V 0A6, Canada. [253]Dipartimento di Scienze Farmacologiche e Biomolecolari, Università di Milano & Centro Cardiologico Monzino, Instituto di Ricovero e Cura a Carattere Scientifico, Milan 20133, Italy. [254]Department of Food Science and Nutrition, Laval University, Quebec, QC G1V 0A6, Canada. [255]Department of Internal Medicine, University Hospital (CHUV) and University of Lausanne, 1011, Switzerland. [256]Department of Nutrition, University of North Carolina, Chapel Hill, North Carolina 27599, USA. [257]Institute of Social and Preventive Medicine (IUMSP), Centre Hospitalier Universitaire Vaudois and University of Lausanne, 1010 Lausanne, Switzerland. [258]Ministry of Health, Victoria, Republic of Seychelles. [259]Lee Kong Chian School of Medicine, Imperial College London and Nanyang Technological University, Singapore, 637553 Singapore, Singapore. [260]Department of Internal Medicine I, Ulm University Medical Centre, D-89081 Ulm, Germany. [261]Department of Clinical Pharmacology, William Harvey Research Institute, Barts and The London School of Medicine and Dentistry, Queen Mary University of London, London EC1M 6BQ, UK. [262]Department of Psychiatry and Psychotherapy, University Medicine Greifswald, HELIOS-Hospital Stralsund, D-17475 Greifswald, Germany. [263]German Center for Neurodegenerative Diseases (DZNE), Rostock, Greifswald, D-17475 Greifswald, Germany. [264]School of Population Health, The University of Western Australia, Nedlands, Western Australia 6009, Australia. [265]Center for Human Genetics, Division of Public Health Sciences, Wake Forest School of Medicine, Winston-Salem, North Carolina 27157, USA. [266]Synlab Academy, Synlab Services GmbH, 68163 Mannheim, Germany. [267]Department of Clinical Genetics, Erasmus MC University Medical Center, 3000 CA Rotterdam, The Netherlands. [268]Department of Medicine, Stanford University School of Medicine, Palo Alto, California 94304, USA. [269]Finnish Diabetes Association, Kirjoniementie 15, FI-33680 Tampere, Finland. [270]Pirkanmaa Hospital District, FI-33521 Tampere, Finland. [271]Center for Non-Communicable Diseases, Karatchi, Pakistan. [272]Department of Medicine, University of Pennsylvania, Philadelphia, Pennsylvania 19104 USA. [273]Helsinki University Central Hospital Heart and Lung Center, Department of Medicine, Helsinki University Central Hospital, FI-00290 Helsinki, Finland. [274]Faculty of Medicine, University of Iceland, Reykjavik 101, Iceland. [275]Instituto de Investigacion Sanitaria del Hospital Universario LaPaz (IdiPAZ), 28046 Madrid, Spain. [276]Diabetes Research Group, King Abdulaziz University, 21589 Jeddah, Saudi Arabia. [277]Centre for Vascular Prevention, Danube-University Krems, 3500 Krems, Austria. [278]Department of Public Health and Clinical Nutrition, University of Eastern Finland, FI-70211 Kuopio, Finland. [279]Research Unit, Kuopio University Hospital, FI-70210 Kuopio, Finland. [280]Durrer Center for Cardiogenetic Research, Interuniversity Cardiology Institute Netherlands-Netherlands Heart Institute, 3501 DG Utrecht, The Netherlands. [281]EPIMED Research Center, Department of Clinical and Experimental Medicine, University of Insubria, Varese I-21100, Italy. [282]Institute of Cellular Medicine, Newcastle University, Newcastle NE1 7RU, UK. [283]Institute of Medical Informatics, Biometry and Epidemiology, Chair of Epidemiology, Ludwig-Maximilians-Universität, D-85764 Munich, Germany. [284]Klinikum Grosshadern, D-81377 Munich, Germany. [285]Institute of Epidemiology I, Helmholtz Zentrum München - German Research Center for Environmental Health, Neuherberg, Germany, D-85764 Neuherberg, Germany. [286]Division of Cancer Epidemiology and Genetics, National Cancer Institute, National Institutes of Health, Bethesda, Maryland 20892, USA. [287]Princess Al-Jawhara Al-Brahim Centre of Excellence in Research of Hereditary Disorders (PACER-HD), King Abdulaziz University, 21589 Jeddah, Saudi Arabia. [288]Albert Einstein College of Medicine, Department of Epidemiology and Population Health, Belfer 1306, New York 10461, USA. [289]Division of Population Health Sciences & Education, St George's, University of London, London SW17 0RE, UK. [290]Department of Human Genetics, University of Michigan, Ann Arbor, Michigan 48109, USA. [291]Queensland Brain Institute, The University of Queensland, Brisbane 4072, Australia. [292]The University of Queensland Diamantina Institute, The Translation Research Institute, Brisbane 4012, Australia. [293]Oxford NIHR Biomedical Research Centre, Oxford University Hospitals NHS Trust, Oxford OX3 7LJ, UK. [294]Carolina Center for Genome Sciences, University of North Carolina at Chapel Hill, Chapel Hill, North Carolina 27599, USA. [295]University of Cambridge Metabolic Research Laboratories, Institute of Metabolic Science, Addenbrooke's Hospital, Cambridge CB2 0QQ, UK. [296]NIHR Cambridge Biomedical Research Centre, Institute of Metabolic Science, Addenbrooke's Hospital, Cambridge CB2 0QQ, UK. [297]The Charles Bronfman Institute for Personalized Medicine, Icahn School of Medicine at Mount Sinai, New York, New York 10029, USA. [298]The Genetics of Obesity and Related Metabolic Traits Program, The Icahn School of Medicine at Mount Sinai, New York, New York 10029, USA. [299]The Mindich Child Health and Development Institute, Icahn School of Medicine at Mount Sinai, New York, New York 10029, USA. [300]Department of Biostatistics, University of Liverpool, Liverpool L69 3GA, UK.

†A list of authors and affiliations appears in the Supplementary Information.
*These authors contributed equally to this work.
§These authors jointly supervised this work.

METHODS

Study overview. Our study included 224,459 individuals of European, east Asian, south Asian and African-American ancestry. The European ancestry arm included 142,762 individuals from 57 cohorts genotyped with genome-wide SNP arrays and 67,326 individuals from 44 cohorts genotyped with the Metabochip[11] (Extended Data Fig. 1 and Supplementary Table 1). The non-European ancestry arm comprised ~1,700 individuals from one cohort of east Asian ancestry, ~3,400 individuals from one cohort of south Asian ancestry, and ~9,200 individuals from six cohorts of African-American ancestry, all genotyped with the Metabochip. There was no overlap between individuals genotyped with genome-wide SNP arrays and Metabochip. For each study, local institutional committees approved study protocols and confirmed that informed consent was obtained. No statistical methods were used to predetermine sample size.

Traits. Our primary trait was WHRadjBMI, the ratio of waist and hip circumferences adjusted for age, age-squared, study-specific covariates if necessary and BMI. For each cohort, residuals were calculated for men and women separately and then transformed by the inverse standard normal function. Cohorts with related men and women provided inverse standard normal transformed sex-combined residuals. For each cohort, the same transformations were applied to other traits: (1) WHR without adjustment for BMI (WHR); (2) waist circumference with (WCadjBMI) and without adjustment for BMI; and (3) hip circumference with (HIPadjBMI) and without adjustment for BMI.

European ancestry meta-analysis for genome-wide SNP array data. Sample and SNP quality control were undertaken within each cohort[44] (Supplementary Table 3). The GWAS scaffold in each cohort was imputed up to CEU haplotypes from HapMap resulting in ~2.5 million SNPs. Each directly typed and imputed SNP passing quality control was tested for association with each trait under an additive model in a linear regression framework (Supplementary Table 3). SNP positions are reported based on NCBI Build 36. For each cohort, sex-specific association summary statistics were corrected for residual population structure using the genomic control inflation factor[45] (median $\lambda_{GC} = 1.01$, range = 0.99–1.08). SNPs were removed before meta-analysis if they had a minor allele count ≤3, deviation from Hardy–Weinberg equilibrium exact $P < 10^{-6}$, directly genotyped SNP call rate <95%, or low imputation quality (below 0.3 for MACH, 0.4 for IMPUTE, and 0.8 for PLINK). Association summary statistics for each trait were combined via inverse-variance weighted fixed-effects meta-analysis and corrected for a second round of genomic control to account for structure between cohorts (Extended Data Fig. 1 and Supplementary Fig. 1).

European ancestry meta-analysis for Metabochip data. Sample and SNP quality control analyses were undertaken in each cohort (Supplementary Table 3). Each SNP passing quality control was tested for association with each trait under an additive model using linear regression. The Metabochip array[11] is enriched, by design, for loci associated with anthropometric and cardiometabolic traits, thus, we based our correction on 4,425 SNPs selected for inclusion based on associations with QT-interval that were not expected to be associated with anthropometric traits (>500 kb from variants on Metabochip[46] for these traits). These study-specific inflation factors had a median $\lambda_{GC} = 1.01$(range 0.93–1.11), with only one study exceeding 1.10. After removing SNPs for quality control as described in the previous section, association summary statistics were combined via inverse-variance weighted fixed-effects meta-analysis and corrected for a second round of genomic control on the basis of QT-interval SNPs to account for structure between cohorts.

European ancestry meta-analyses. Association summary statistics from the two parts of the European ancestry arm were combined via inverse-variance weighted fixed-effects meta-analysis using METAL[47] with no further genomic control correction. Results were reported for SNPs with a sex-combined sample size ≥50,000. The meta-analyses were repeated for men and women separately for each trait. Analyses were corrected for population structure within each sex. The meta-analysis of WHRadjBMI in men included up to 93,480 individuals, and in women up to 116,742 individuals.

Meta-analyses of studies of all ancestries. Sample and SNP quality control, tests of association, genomic control correction (median $\lambda_{GC} = 1.01$, range = 0.90–1.17, with only one study exceeding 1.10), and meta-analyses were performed as described above. Association summary statistics from the European and non-European ancestry meta-analyses were combined via inverse-variance weighted fixed-effects meta-analysis without further genomic control correction.

Heterogeneity. For each lead SNP, we tested for sex differences based on the sex-specific beta estimates and standard errors, while accounting for potential correlation between estimates as previously described[10]. Similarly, we tested for potential differences in effects between European and non-European samples, comparing the effects from GWAS+Metabochip data for Europeans and Metabochip data for non-Europeans, and we tested for differences between population-based studies and samples ascertained on diabetes status, and cardiovascular disease, or both. In assessing effects of ascertainment overall, we compared effects in seven subsets of our study sample using population-based studies (that is, those not ascertained on any phenotype) as the referent population: (1) all studies ascertained on any phenotype, (2) T2D cases, (3) T2D controls, (4) T2D cases plus controls, (5) CAD cases, (6) CAD controls and (7) CAD cases plus controls. We evaluated significance for heterogeneity tests within each comparison using a Bonferroni-corrected P value of $0.05/49 = 0.05/49 = 1.02 \times 10^{-3}$ as well as an FDR threshold[48] of <5% (Supplementary Table 28). Between-study heterogeneity in all meta-analyses was assessed using I^2 statistics[49].

Heritability and genetic and phenotypic correlations of waist traits. We calculated the heritability and genetic correlations of several central obesity traits using variance component models[50,51] in the Framingham Heart Study (FHS) and TwinGene study. In this approach, the phenotypic variance is decomposed into additive genetic, non-additive genetic, and environmental sources of variation (including model error), and for sets of traits, the covariances between traits. We report narrow sense heritability (h^2), the ratio of the additive genetic variance to the total phenotypic variance. Sex-specific inverse normal trait residuals, adjusted for age (and cohort in FHS), were used to estimate heritability separately in men and women, using variance components analysis in SOLARv.4.2.7 (FHS)[52] or Mx1.703 (TwinGene)[53]. Additionally, the sex-specific residuals were used to conduct bivariate quantitative variance component genetic analyses that calculate genetic and environmental correlations between traits. The genetic correlations obtained are estimates of the additive effects of shared genes, and a genetic correlation significantly different from zero suggests a direct influence of the same genes on more than one trait. Similarly, significant environmental correlations suggest shared environmental effects.

We estimated sex-stratified correlations between all waist traits, as well as BMI, height, and weight in TwinGene, FHS, KORA and EGCUT. In TwinGene and FHS, age-adjusted Pearson correlations were used; in EGCUT and KORA, correlations were adjusted for age and age-squared.

European ancestry approximate conditional analyses. To evaluate the evidence for multiple association signals within identified loci, we performed approximate conditional analyses of sex-combined, women-specific and men-specific data as implemented in the GCTA software[14,54]. This approach makes use of association summary statistics from the combined European ancestry meta-analysis and a reference data set of individual-level genotype data to estimate LD between variants and hence also the approximate correlation between allelic effect estimates in a joint association model.

To evaluate robustness of the GCTA results, we performed analyses using two reference data sets: Prospective Investigation of the Vasculature in Uppsala Seniors (PIVUS) consisting of 949 individuals from Uppsala County, Sweden, with both GWAS and Metabochip genotype data; and Atherosclerosis Risk in Communities (ARIC) consisting of 6,654 individuals of European descent from four communities in the United States with GWAS data. Both GWAS data sets were imputed using data from phase II of the International HapMap Project[55]. Results shown use the PIVUS reference data set because Metabochip genotypes are available (see a comparison in the Supplementary Note). Assuming that the LD correlations between SNPs more than 10 megabases (Mb) away are zero, and using each reference data set in turn, we performed a genome-wide stepwise selection procedure to select associated SNPs one-by-one at a $P < 5 \times 10^{-8}$. For each locus at which multiple association signals were observed in the sex-combined, women-, and/or men-specific data, the SNPs selected by GCTA as independently associated with WHRadjBMI in any of the three meta-analyses are reported, with the SNP identified in the sex-combined analysis taken by default when proxies are identified in the women- and/or men-specific analyses. For SNPs not selected by a particular joint conditional analysis, but identified by either of the other two analyses, summary statistics were calculated for association analysis of the SNP conditioned on the GCTA-selected SNP(s).

Genetic risk score. We calculated a genetic risk score for each individual in the population-based KORA study (1,670 men and 1,750 women) using the 49 identified variants, weighted by the allelic effect from the European ancestry meta-analyses of WHRadjBMI. Sex-combined scores were computed on the basis of the sex-combined meta-analysis. Sex-stratified scores were calculated on the basis of men- and women-specific meta-analyses, in which SNPs not achieving nominal significance in the respective sex ($P \geq 0.05$) were excluded. For each individual, the sex-combined and sex-stratified risk scores were rounded to the nearest integer for plotting. Risk scores were then tested for association with WHRadjBMI using linear regression.

Explained variance. We calculated the variance explained by a single SNP as:

$$2 \bullet \mathrm{MAF} \bullet (1 - \mathrm{MAF}) \bullet \frac{\beta^2}{\mathrm{Var}(Y)}$$

in which MAF is the minor allele frequency, β is the SNP effect estimate computed by meta-analysis, and $\mathrm{Var}(Y)$ is the variance of the phenotype Y as it went into the study-specific association testing. To derive the total variance explained by a set of

independent SNPs, we computed the sum of single-SNP explained variances under the assumption of independent contributions.

To estimate the polygenic variance explained by all HapMap SNPs, we used the all-SNP estimation approach implemented in GCTA and analysed individuals in the ARIC and TwinGene cohorts, including the first 20 principal components as fixed covariates. After removing one of each pair of individuals with estimated genetic relatedness >0.025, 11,898 unrelated individuals with WHRadjBMI were available.

Fine-mapping analyses. We considered each identified locus, defined as 500 kb upstream and downstream of the lead SNP, and computed 99% credible intervals using a Bayesian approach. On the basis of association summary statistics from the European ancestry, non-European ancestry, or all ancestries sex-combined meta-analyses, we calculated an approximate Bayes' factor[56] in favour of association, given by:

$$\mathrm{BF}_j = \frac{\sqrt{1-R_j}}{\exp\left(-\frac{R_j\beta_j^2}{2\sigma_j^2}\right)}$$

in which β_j is the allelic effect of the jth SNP, with corresponding standard error σ_j, and $R_j = 0.04/(\sigma_j^2 + 0.04)$, which incorporates a $N(0,0.2^2)$ prior for β_j. This prior gives high probability to small effect sizes, and only small probability to large effect sizes. We then calculated the posterior probability that the jth SNP is causal by:

$$\varphi_j = \frac{\mathrm{BF}_j}{\sum_k \mathrm{BF}_k}$$

in which the summation in the denominator is over all SNPs passing quality control across the locus. We compared the meta-analysis results and credible sets of SNPs likely to contain the causal variant as described[57]. Assuming a single causal variant at each locus, a 99% credible set of variants was then constructed by: (1) ranking all SNPs according to their Bayes' factor; and (2) combining ranked SNPs until their cumulative posterior probability exceeded 0.99. For each locus, we calculated the number of SNPs contained within the 99% credible sets, and the length of the genomic interval covered by these SNPs.

Comparison of loci across traits. To determine whether the identified loci were also associated with any of 22 cardio-metabolic traits, we obtained association data from meta-analysis consortia DIAGRAM (T2D)[58], CARDIoGRAM-C4D (CAD)[59], ICBP (diastolic and systolic blood pressure)[60], GIANT (BMI, height)[36,37], GLGC (HDL, LDL, and triglycerides)[61], MAGIC (fasting glucose, fasting insulin, fasting insulin adjusted for BMI, and two-hour glucose)[62–64], ADIPOGen (BMI-adjusted adiponectin)[65], CKDgen (urine albumin-to-creatinine ratio (UACR), estimated glomerular filtration rate (eGFR), and overall CKD)[66,67], ReproGen (age at menarche, age at menopause)[68,69], and GEFOS (bone mineral density)[70]; others provided association data for IgA nephropathy[71] (also K.K., M.C., R.P.L. and A.G.G., unpublished data) and for endometriosis (stage B cases only)[72]. Proxies ($r^2 > 0.8$ in CEU) were used when an index SNP was unavailable.

We also searched the NHGRI GWAS catalogue for previous SNP-trait associations near our lead SNPs[73]. We supplemented the catalogue with additional genome-wide significant SNP-trait associations from the literature[13,70,74–80]. We used PLINK to identify SNPs within 500 kb of lead SNPs using 1000 Genomes Project pilot I genotype data and LD (r^2) values from CEU[81,82]; for rs7759742, HapMap release 22 CEU data[81,83] were used. All SNPs within the specified regions were compared with the NHGRI GWAS catalogue[16].

Enrichment of concordant cross-trait associations and effects. To evaluate whether the alleles associated with increased WHRadjBMI at the 49 identified SNPs convey effects for any of the 22 cardiometabolic traits, we conducted meta-regression analyses of the beta-estimates on these metabolic outcomes from other consortia with the beta-estimates for WHRadjBMI in our data[65].

On the basis of the association data across traits, we generated a matrix of Z-scores by dividing the association betas for each of the 49 WHRadjBMI SNPs for each of 22 traits by their respective standard errors. The traits did not include WHRadjBMI or nephropathy in Chinese subjects, but did include HIPadjBMI and WCadjBMI. Each Z-score was made positive if the original trait-increasing allele also increased the look-up trait and negative if not. Missing associations with were assigned a value of zero. We performed unsupervised hierarchical clustering of the Z score matrix in R using the default settings of the 'heatplot' function from the made4 library (version 1.20.0), agglomerating clusters using average linkage and Pearson correlation metric distance. The rows and columns of matrix values were each automatically scaled to range from 3 to −3. Confidence in the hierarchical clustering was assessed by bootstrap analysis (10,000 resamplings) using the R package 'pvclust'[84].

Identification of candidate functional variants. The 1000 Genomes CEU pilot data were queried for SNPs within 500 kb and in LD ($r^2 > 0.7$, an arbitrary threshold) with any index SNP. All identified variants were then annotated based on RefSeq transcripts using Annovar to identify potential nonsynonymous variants near identified association signals. The distance between each variant and the nearest transcription start site were calculated using gene annotations from GENCODE (v.12).

To investigate whether SNPs in LD with index SNPs are also in LD with common copy number variants (CNVs), we extracted waist trait association results for a list of SNP proxies that are in high LD ($r^2 > 0.8$, CEU) with CNVs in European populations as described previously[7]. Altogether 6,200 CNV-tagging SNPs were used, which are estimated collectively to capture >40% of CNVs >1 kb in size.

eQTLs. We examined our lead SNPs in eQTL data sets from several sources (Supplementary Note) for *cis* effects significant at $P < 10^{-5}$. We then checked if the trait-associated SNP also had the strongest association with the expression level of its corresponding transcript. If not, we identified a nearby SNP that had a stronger association with expression (peak transcript SNP) of that transcript. To check whether effects of the peak transcript SNP and waist trait-associated SNP overlapped, we conducted conditional analyses to estimate associations between the waist-associated SNP and transcript level when the peak-transcript-associated SNP was also included in the model, and vice versa. If the association for the expression-associated SNP was not significant ($P > 0.05$) when conditioned on the waist-associated SNP, we concluded that the waist-associated SNP is likely to explain a substantial proportion of the variance in gene transcript levels in the region. For SNPs that passed these criteria in either women or men eQTL data sets from deCODE, we investigated sex heterogeneity in gene transcript levels for whole blood (312 men, 435 women) and subcutaneous adipose tissue (252 men, 351 women) based on the sex-specific beta estimates and standard errors, while accounting for potential correlation between the sex-specific associations[8].

Epigenomic regulatory element overlap with individual variants. We examined overlap of regulatory elements with the 68 trait-associated variants and variants in LD with them ($r^2 > 0.7$, 1000 Genomes phase 1 version 2 EUR[85]), totalling 1,547 variants. We obtained regulatory element data sets from the ENCODE Consortium[24] and Roadmap Epigenomics Project[25] corresponding to eight tissues selected based on a current understanding of WHRadjBMI pathways. The 226 regulatory element data sets included experimentally identified regions of open chromatin (DNase-seq, FAIRE-seq), histone modification (H3K4me1, H3K27ac, H3K4me3, H3K9ac and H3K4me2), and transcription factor binding (Supplementary Table 17). When available, we downloaded data processed during the ENCODE Integrative Analysis[24]. We processed Roadmap Epigenomics sequencing data with multiple biological replicates using MACS2 (ref. 86) and the same Irreproducible Discovery Rate pipeline used in the ENCODE Integrative Analysis. Roadmap Epigenomics data with only a single replicate was processed using MACS2 alone.

Global enrichment of WHRadjBMI-associated loci in epigenomic data sets. We performed permutation-based tests in a subset of 60 open chromatin (DNase-seq) and histone modification (H3K27ac, H3K4me1, H3K4me3 and H3K9ac) data sets to identify global enrichment of the WHRadjBMI-associated loci. We matched the index SNP at each locus with 500 variants having no evidence of association ($P > 0.5$, ~1.2 million total variants) with a similar distance to the nearest gene (±11,655 bp), number of variants in LD (±8 variants), and minor allele frequency. Using these pools, we created 10,000 sets of control variants for each of the 49 loci and identified variants in LD ($r^2 > 0.7$) and within 1 Mb. For each SNP set, we calculated the number of loci with at least one variant located in a regulatory region under the assumption that one regulatory variant is responsible for each association signal. We initially calculated an enrichment P value by finding the proportion of control sets for which as many or more loci overlap a regulatory element than the set of associated loci. For increased P value accuracy, we estimated the P value assuming a sum of binomial distributions to represent the number of index SNPs or their LD proxies that overlap a regulatory data set compared to the 500 matched control sets.

GRAIL. Gene Relationships Among Implicated Loci (GRAIL)[19] is a text-mining algorithm that evaluates the degree of relatedness among genes within trait regions. Using PubMed abstracts, a subset of genes enriched for relatedness and a set of keywords that suggest putative pathways are identified. To avoid potential bias from papers investigating candidate genes stimulated by GWAS, we restricted our search to abstracts published before 2006. We tested for enrichment of connectivity in the independent SNPs that were significant in our study at $P < 10^{-5}$.

MAGENTA. To investigate whether pathways including predefined sets of genes were enriched in the lower part of the gene P value distribution for WHRadjBMI, we performed a pathway analysis using Magenta 2.4 (ref. 20) and SNPs present in both the Metabochip and GWAS meta-analyses. SNPs were assigned to a gene if within 110 kb upstream or 40 kb downstream of the transcript's boundaries. The most significant SNP P value within this interval was adjusted for putative confounders (gene size, number of SNPs in a gene, LD pattern) using stepwise linear

regression, creating a gene association score. If the same SNP was assigned to multiple genes, only the gene with the lowest gene score was kept. The *HLA* region was removed from further analyses owing to its high LD structure and gene density. Each gene was then assigned pathway terms using Gene Ontology (GO), PANTHER, Ingenuity and Kyoto Encyclopedia of Genes and Genomes (KEGG)[87–90]. Finally, the genes were ranked based on their gene association score, and a modified gene-set enrichment analysis using MAGENTA was performed. This analysis tested for enrichment of gene association score ranks above a given rank cutoff (including 5% of all genes) in a gene-set belonging to a predefined pathway term, compared to multiple, equally sized gene-sets that were randomly sampled from all genes in the genome. Around 10,000–1,000,000 gene-set permutations were performed.

DEPICT. This method is described in detail elsewhere[23,36]. In brief, DEPICT uses gene expression data derived from a panel of 77,840 expression arrays[91], 5,984 molecular pathways (based on 169,810 high-confidence experimentally derived protein–protein interactions[92]), 2,473 phenotypic gene sets (based on 211,882 gene-phenotype pairs from the Mouse Genetics Initiative[93]), 737 reactome pathways[94], 184 KEGG pathways[95], and 5,083 GO terms[19]. DEPICT uses the expression data to reconstitute the protein–protein interaction gene sets, mouse phenotype gene sets, reactome pathway gene sets, KEGG pathway gene sets, and GO term gene sets. To avoid biasing the identification of genes and pathways covered by SNPs on the Metabochip, analyses were restricted to GWAS cohort data and included 226 WHRadjBMI SNPs in 78 non-overlapping loci with sex-combined $P < 10^{-5}$. We used DEPICT to map genes to associated WHRadjBMI loci, which then allowed us to (1) systematically identify the most likely causal gene(s) in a given associated region, (2) identify reconstituted gene sets that were enriched in genes from associated regions, and (3) identify tissue and cell type annotations in which genes from associated regions were highly expressed. Associated regions were defined by all genes residing within LD ($r^2 > 0.5$) distance of the WHRadjBMI-associated index SNPs. Overlapping regions were merged, and SNPs that mapped near to or within the HLA region were excluded. The 93 WHRadjBMI SNPs with $P < 10^{-5}$ (clumping thresholds: HapMap release 27 CEU $r^2 = 0.01$, 500 kb) resulted in 78 non-overlapping regions. GWAS+Metabochip index SNPs were annotated with DEPICT-prioritized genes if the DEPICT (GWAS-only) SNP was located within 500 kb. To mark related gene sets, we first quantified significant gene sets' pairwise overlap using a non-probabilistic version of the reconstituted gene sets and the Jaccard index measure. Groups of gene sets with mutual Jaccard indices >0.25 were subsequently referred to as meta gene sets and named by the most significant gene set in the group (Supplementary Table 18 and Fig. 2a). In Fig. 2a, b, gene sets with similarities between 0.1 and 0.25 were connected by an edge that was scaled according to degree of similarity. The Cytoscape tool was used to construct parts of Fig. 2 (ref. 96). In Fig. 2c, we show the significance of all cell type annotations and annotations that were categorized as 'tissues' at the outermost level of the Medical Subject Heading ontology.

44. Winkler, T. W. *et al.* Quality control and conduct of genome-wide association meta-analyses. *Nature Protocols* **9,** 1192–1212 (2014).
45. Devlin, B. & Roeder, K. Genomic control for association studies. *Biometrics* **55,** 997–1004 (1999).
46. Buyske, S. *et al.* Evaluation of the metabochip genotyping array in African Americans and implications for fine mapping of GWAS-identified loci: the PAGE study. *PLoS ONE* **7,** e35651 (2012).
47. Willer, C. J., Li, Y. & Abecasis, G. R. METAL: fast and efficient meta-analysis of genomewide association scans. *Bioinformatics* **26,** 2190–2191 (2010).
48. Benjamini, Y. & Hochberg, Y. Controlling the false discovery rate: a practical and powerful approach to multiple testing. *J. R. Stat. Soc. Series B Stat. Methodol.* **57,** 289–300 (1995).
49. Higgins, J. P. & Thompson, S. G. Quantifying heterogeneity in a meta-analysis. *Stat. Med.* **21,** 1539–1558 (2002).
50. Neale, M. C., Cardon, L. R. & North Atlantic Treaty Organization. *Methodology for Genetic Studies of Twins and Families* (Kluwer Academic Publishers, 1992).
51. Falconer, D. S. *Introduction to Quantitative Genetics* 3rd edn (Oliver and Boyd, 1990).
52. Almasy, L. & Blangero, J. Multipoint quantitative-trait linkage analysis in general pedigrees. *Am. J. Hum. Genet.* **62,** 1198–1211 (1998).
53. Neale, M. C. *MX: Statistical Modeling* 4th edn (Department of Psychiatry, 1997).
54. Yang, J., Lee, S. H., Goddard, M. E. & Visscher, P. M. GCTA: a tool for genome-wide complex trait analysis. *Am. J. Hum. Genet.* **88,** 76–82 (2011).
55. Frazer, K. A. *et al.* A second generation human haplotype map of over 3.1 million SNPs. *Nature* **449,** 851–861 (2007).
56. Wakefield, J. A Bayesian measure of the probability of false discovery in genetic epidemiology studies. *Am. J. Hum. Genet.* **81,** 208–227 (2007).
57. Wellcome Trust Case Control Consortium. Bayesian refinement of association signals for 14 loci in 3 common diseases. *Nature Genet.* **44,** 1294–1301 (2012).
58. Morris, A. P. *et al.* Large-scale association analysis provides insights into the genetic architecture and pathophysiology of type 2 diabetes. *Nature Genet.* **44,** 981–990 (2012).
59. Deloukas, P. *et al.* Large-scale association analysis identifies new risk loci for coronary artery disease. *Nature Genet.* **45,** 25–33 (2013).
60. Ehret, G. B. *et al.* Genetic variants in novel pathways influence blood pressure and cardiovascular disease risk. *Nature* **478,** 103–109 (2011).
61. Global Lipids Genetics Consortium. Discovery and refinement of loci associated with lipid levels. *Nature Genet.* **45,** 1274–1283 (2013).
62. Scott, R. A. *et al.* Large-scale association analyses identify new loci influencing glycemic traits and provide insight into the underlying biological pathways. *Nature Genet.* **44,** 991–1005 (2012).
63. Manning, A. K. *et al.* A genome-wide approach accounting for body mass index identifies genetic variants influencing fasting glycemic traits and insulin resistance. *Nature Genet.* **44,** 659–669 (2012).
64. Saxena, R. *et al.* Genetic variation in *GIPR* influences the glucose and insulin responses to an oral glucose challenge. *Nature Genet.* **42,** 142–148 (2010).
65. Dastani, Z. *et al.* Novel loci for adiponectin levels and their influence on type 2 diabetes and metabolic traits: a multi-ethnic meta-analysis of 45,891 individuals. *PLoS Genet.* **8,** e1002607 (2012).
66. Pattaro, C. *et al.* Genome-wide association and functional follow-up reveals new loci for kidney function. *PLoS Genet.* **8,** e1002584 (2012).
67. Böger, C. A. *et al. CUBN* is a gene locus for albuminuria. *J. Am. Soc. Nephrol.* **22,** 555–570 (2011).
68. Stolk, L. *et al.* Meta-analyses identify 13 loci associated with age at menopause and highlight DNA repair and immune pathways. *Nature Genet.* **44,** 260–268 (2012).
69. Elks, C. E. *et al.* Thirty new loci for age at menarche identified by a meta-analysis of genome-wide association studies. *Nature Genet.* **42,** 1077–1085 (2010).
70. Estrada, K. *et al.* Genome-wide meta-analysis identifies 56 bone mineral density loci and reveals 14 loci associated with risk of fracture. *Nature Genet.* **44,** 491–501 (2012).
71. Gharavi, A. G. *et al.* Genome-wide association study identifies susceptibility loci for IgA nephropathy. *Nature Genet.* **43,** 321–327 (2011).
72. Painter, J. N. *et al.* Genome-wide association study identifies a locus at 7p15.2 associated with endometriosis. *Nature Genet.* **43,** 51–54 (2011).
73. Hindorff, L. A. *et al.* Potential etiologic and functional implications of genome-wide association loci for human diseases and traits. *Proc. Natl Acad. Sci. USA* **106,** 9362–9367 (2009).
74. Kamatani, Y. *et al.* Genome-wide association study of hematological and biochemical traits in a Japanese population. *Nature Genet.* **42,** 210–215 (2010).
75. Franke, A. *et al.* Genome-wide meta-analysis increases to 71 the number of confirmed Crohn's disease susceptibility loci. *Nature Genet.* **42,** 1118–1125 (2010).
76. Sawcer, S. *et al.* Genetic risk and a primary role for cell-mediated immune mechanisms in multiple sclerosis. *Nature* **476,** 214–219 (2011).
77. Wang, K. S., Liu, X. F. & Aragam, N. A genome-wide meta-analysis identifies novel loci associated with schizophrenia and bipolar disorder. *Schizophr. Res.* **124,** 192–199 (2010).
78. Cirulli, E. T. *et al.* Common genetic variation and performance on standardized cognitive tests. *Eur. J. Hum. Genet.* **18,** 815–820 (2010).
79. Gieger, C. *et al.* New gene functions in megakaryopoiesis and platelet formation. *Nature* **480,** 201–208 (2011).
80. Need, A. C. *et al.* A genome-wide study of common SNPs and CNVs in cognitive performance in the CANTAB. *Hum. Mol. Genet.* **18,** 4650–4661 (2009).
81. Purcell, S. *et al.* PLINK: a tool set for whole-genome association and population-based linkage analyses. *Am. J. Hum. Genet.* **81,** 559–575 (2007).
82. The 1000 Genomes Project Consortium. A map of human genome variation from population-scale sequencing. *Nature* **467,** 1061–1073 (2010).
83. The International HapMap Project. *Nature* **426,** 789–796 (2003).
84. Suzuki, R. & Shimodaira, H. Pvclust: an R package for assessing the uncertainty in hierarchical clustering. *Bioinformatics* **22,** 1540–1542 (2006).
85. 1000 Genomes Project Consortium. An integrated map of genetic variation from 1,092 human genomes. *Nature* **491,** 56–65 (2012).
86. Feng, J., Liu, T., Qin, B., Zhang, Y. & Liu, X. S. Identifying ChIP-seq enrichment using MACS. *Nature Protocols* **7,** 1728–1740 (2012).
87. Ashburner, M. *et al.* Gene ontology: tool for the unification of biology. The Gene Ontology Consortium. *Nature Genet.* **25,** 25–29 (2000).
88. Mi, H. & Thomas, P. PANTHER pathway: an ontology-based pathway database coupled with data analysis tools. *Methods Mol. Biol.* **563,** 123–140 (2009).
89. Jimenez-Marin, A., Collado-Romero, M., Ramirez-Boo, M., Arce, C. & Garrido, J. J. Biological pathway analysis by ArrayUnlock and Ingenuity Pathway Analysis. *BMC Proc.* **3,** S6 (2009).
90. Kanehisa, M. & Goto, S. KEGG: Kyoto encyclopedia of genes and genomes. *Nucleic Acids Res.* **28,** 27–30 (2000).
91. Fehrmann, R. S. *et al.* Gene expression analysis identified global gene dosage sensitivity in cancer. *Nature Genet.* **47,** 115–125 (2015).
92. Lage, K. *et al.* A human phenome-interactome network of protein complexes implicated in genetic disorders. *Nature Biotechnol.* **25,** 309–316 (2007).
93. Bult, C. J. *et al.* Mouse genome informatics in a new age of biological inquiry. *IEEE Int. Symposium Bio-Informatics Biomedical Engineering* 29–32 (2000).
94. Croft, D. *et al.* Reactome: a database of reactions, pathways and biological processes. *Nucleic Acids Res.* **39,** D691–D697 (2011).
95. Kanehisa, M., Goto, S., Sato, Y., Furumichi, M. & Tanabe, M. KEGG for integration and interpretation of large-scale molecular data sets. *Nucleic Acids Res.* **40,** D109–D114 (2012).
96. Saito, R. *et al.* A travel guide to Cytoscape plugins. *Nature Methods* **9,** 1069–1076 (2012).

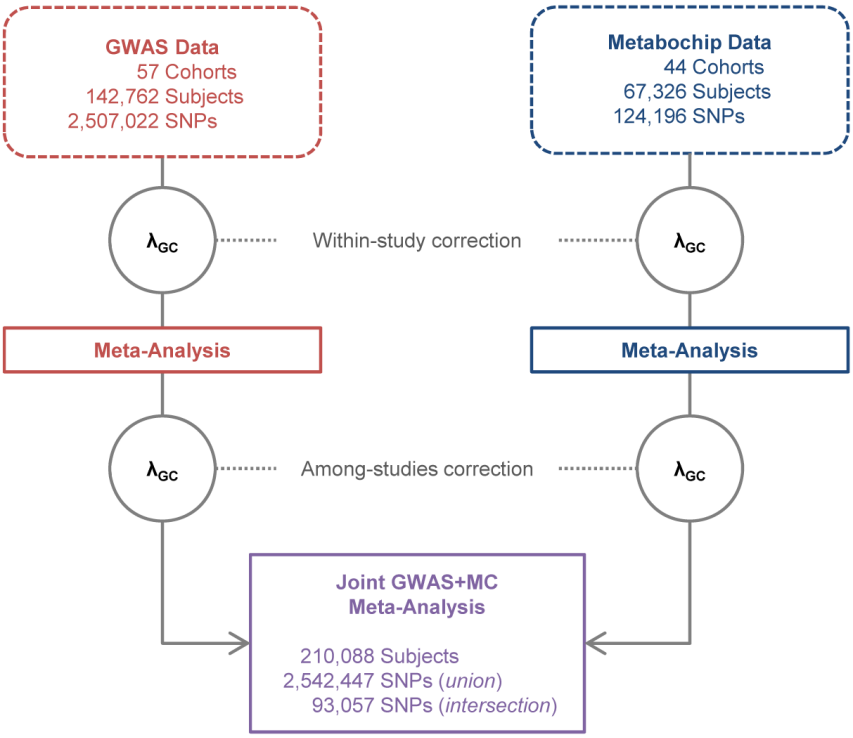

Extended Data Figure 1 | Overall WHRadjBMI meta-analysis study design. Data (dashed lines) and analyses (solid lines) related to the GWAS cohorts for WHRadjBMI are coloured red and those related to the Metabochip (MC) cohorts are coloured blue. The two genomic control (λ_{GC}) corrections (within-study and among-studies) performed on associations from each data set are represented by grey-outlined circles. The λ_{GC} corrections for the GWAS meta-analysis were based on all SNPs and the λ_{GC} corrections for the Metabochip meta-analysis were based on a null set of 4,319 SNPs previously associated with QT interval. The joint meta-analysis of the GWAS and Metabochip data sets is coloured purple. All SNP counts reflect a sample size filter of $n \geq 50{,}000$ subjects. Additional WHRadjBMI meta-analyses included Metabochip data from up to 14,371 subjects of east Asian, south Asian or African-American ancestry from eight cohorts. Counts for the meta-analyses of waist circumference, hip circumference, and their BMI-adjusted counterparts (WCadjBMI and HIPadjBMI) differ from those of WHRadjBMI because some cohorts only had phenotype data available for one type of body circumference measurement (see Supplementary Table 2).

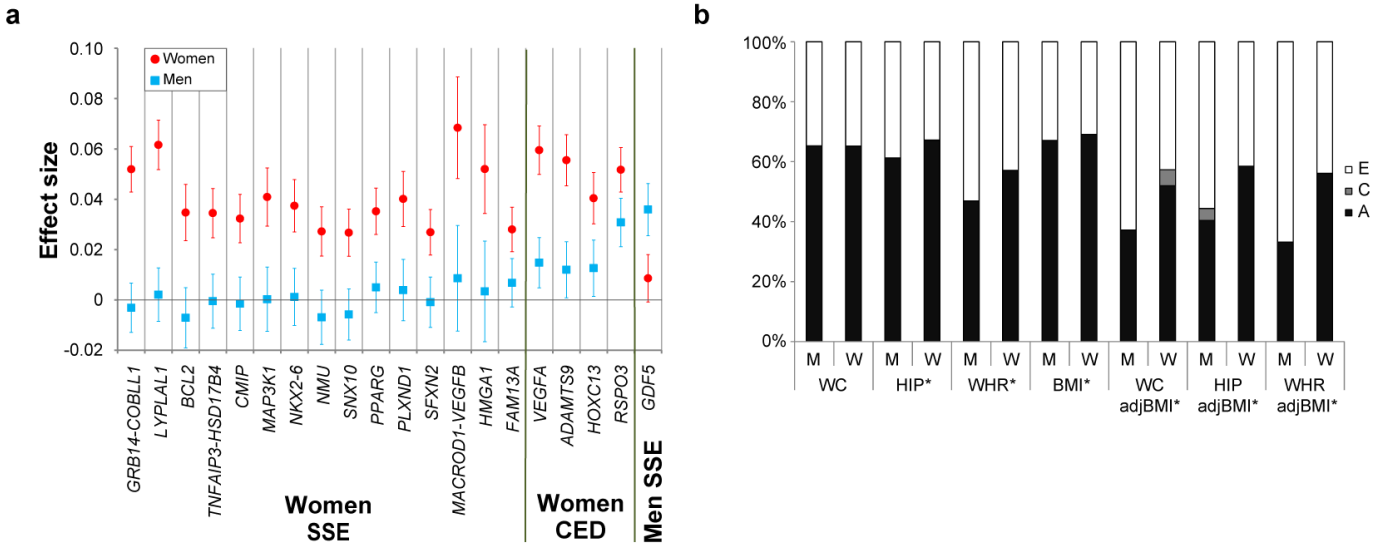

c

	Men		Women	
Trait	**Framingham Heart Study**	**TWINGENE**	**Framingham Heart Study**	**TWINGENE**
WCadjBMI	0.6379	0.5760	0.5036	0.4160
WHRadjBMI	0.0367	-0.0150	0.0052	0.0090
HIPadjBMI	0.8168	0.7110	0.7223	0.6310

Extended Data Figure 2 | Women- and men-specific effects, phenotypic variances and genetic correlations. a, Figure showing effect beta estimates for the 20 WHRadjBMI SNPs showing significant evidence of sexual dimorphism. Sex-specific effect betas and 95% confidence intervals for SNPs associated with WHRadjBMI are shown as red circles and blue squares for women and men, respectively. Sample sizes, comprising more than 73,576 men and 96,182 women, are listed in Table 1. The SNPs are classified into three categories: (1) those showing a women-specific effect ('women SSE'), namely a significant effect in women and no effect in men ($P_{women} < 5 \times 10^{-8}$, $P_{men} \geq 0.05$), (2) those showing a pronounced women effect ('women CED'), namely a significant effect in women and a less significant but directionally consistent effect in men ($P_{women} < 5 \times 10^{-8}$, $5 \times 10^{-8} < P_{men} \leq 0.05$); and (3) those showing a men-specific effect ('men SSE'), namely a significant effect in men and no effect in women ($P_{men} < 5 \times 10^{-8}$, $P_{women} \geq 0.05$). Within each of the three categories, the loci were sorted by increasing P value of sex-based heterogeneity in the effect betas. **b**, Figure showing standardized sex-specific phenotypic variance components for six waist-related traits. Values are shown in men (M) and women (W) from the Swedish Twin Registry ($n = 11,875$). The ACE models are decomposed into additive genetic components (A) shown in black, common environmental components (C) in grey, and non-shared environmental components (E) in white. Components are shown for waist circumference (WC), hip circumference (HIP), WHR, WCadjBMI, HIPadjBMI and WHRadjBMI. When the 'A' component is different in men and women with $P < 0.05$ for a given trait, its name is marked with an asterisk. **c**, Genetic correlations of waist-related traits with height, adjusted for age and BMI. Genetic correlations of three traits with height were based on variance component models in the Framingham Heart Study and TwinGene study (see Methods).

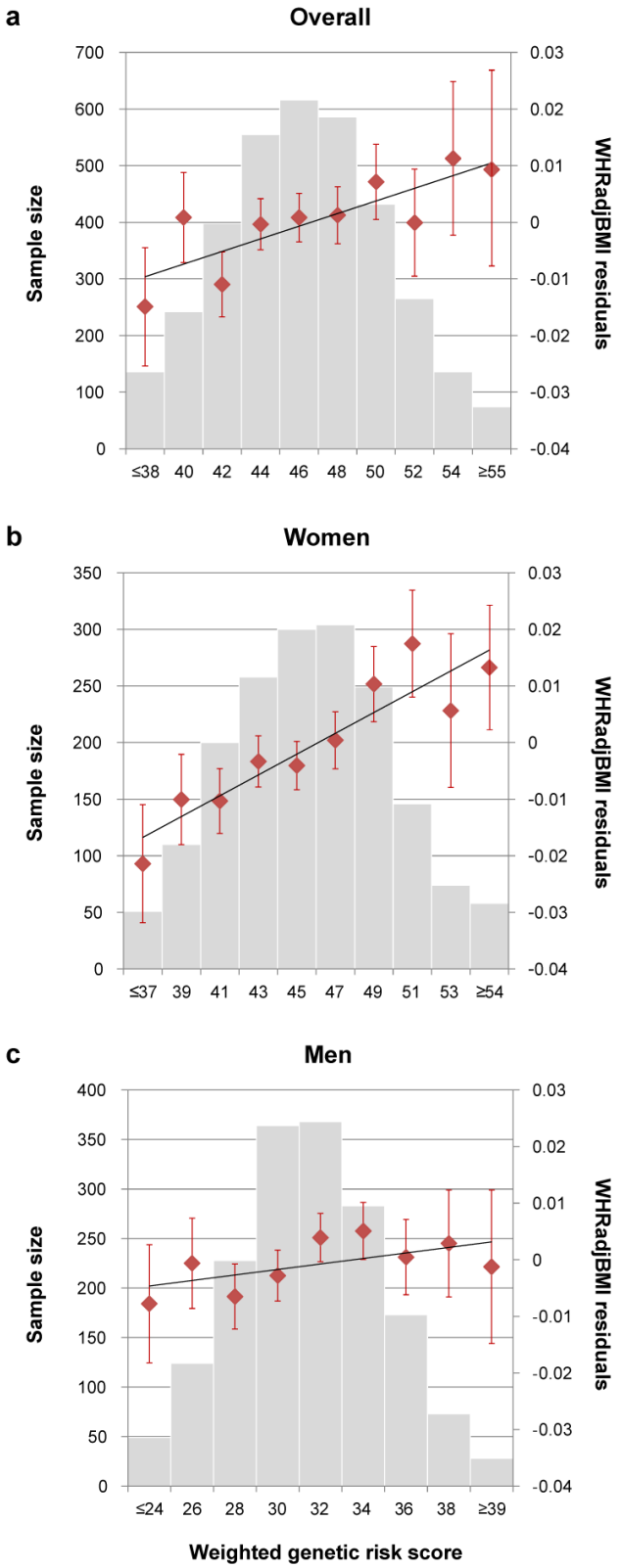

Extended Data Figure 3 | Cumulative genetic risk scores for WHRadjBMI applied to the KORA study cohort. **a**, All subjects ($n = 3,440$, $P_{trend} = 6.7 \times 10^{-4}$). **b**, Only women ($n = 1,750$, $P_{trend} = 1.0 \times 10^{-11}$). **c**, Only men ($n = 1,690$, $P_{trend} = 0.02$). Each genetic risk score illustrates the joint effect of the WHRadjBMI-increasing alleles of the 49 identified variants from Table 1 weighted by the relative effect sizes from the applicable sex-combined or sex-specific meta-analysis. The mean WHRadjBMI residual and 95% confidence interval is plotted for each genetic risk score category (red dots). The histograms show each genetic risk score is normally distributed in KORA (grey bars).

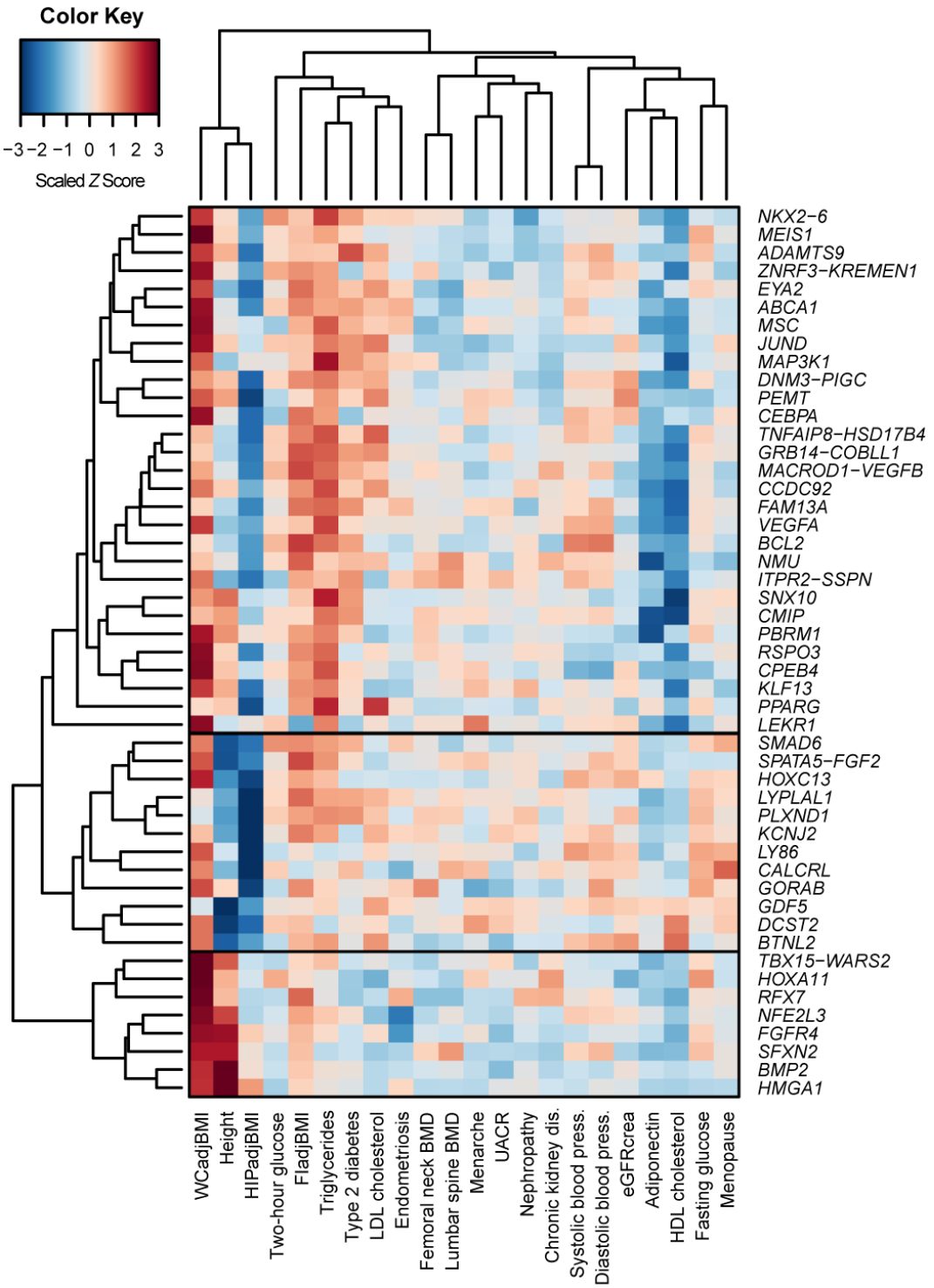

Extended Data Figure 4 | Heat map of unsupervised hierarchical clustering of the effects of 49 WHRadjBMI SNPs on 22 anthropometric and metabolic traits and diseases. The matrix of *Z*-scores representing the set of associations was scaled by row (locus name) and by column (trait) to range from −3 to 3. Negative values (blue) indicate that the WHRadjBMI-increasing allele was associated with decreased values of the trait and positive values (red) indicate that this allele was associated with increased values of the trait. Sample sizes for the associations are listed in Supplementary Table 8. Dendrograms indicating the clustering relationships are shown to the left and above the heat map. The WHRadjBMI-increasing alleles at the 49 lead SNPs segregate into three major clusters comprised of alleles that associate with: (1) larger WCadjBMI and smaller HIPadjBMI ($n = 30$ SNPs); (2) taller stature and larger WCadjBMI ($n = 8$ SNPs); and (3) shorter stature and smaller HIPadjBMI ($n = 11$ SNPs). The three visually identified SNP clusters could be statistically distinguished with >90% confidence. Alleles of the first cluster were predominantly associated with lower high density lipoprotein (HDL) cholesterol and with higher triglycerides and fasting insulin adjusted for BMI (FIadjBMI). BMD, bone mineral density; eGFRcrea, estimated glomerular filtration rate based on creatinine; LDL cholesterol, low-density lipoprotein cholesterol; UACR, urine albumin-to-creatinine ratio.

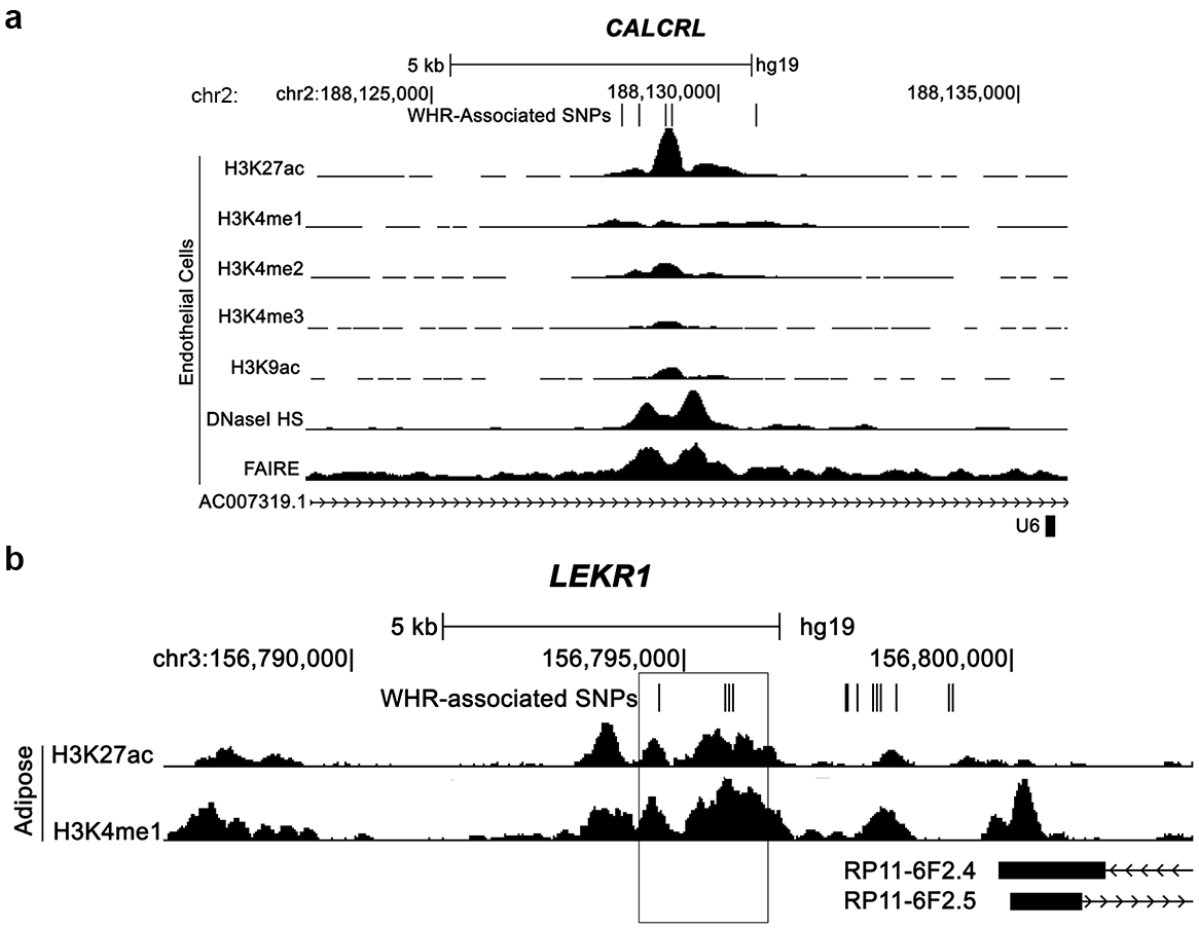

Extended Data Figure 5 | Regulatory element overlap with WHRadjBMI-associated loci. **a**, Five variants associated with WHRadjBMI and located ~77 kb upstream of the first *CALCRL* transcription start site overlap regions with genomic evidence of regulatory activity in endothelial cells. **b**, Five WHRadjBMI variants, including rs8817452, in a 1.1-kb region (box) ~250 kb downstream of the first *LEKR1* transcription start site overlap evidence of active enhancer activity in adipose nuclei. Signal enrichment tracks are from the ENCODE Integrative Analysis and the Roadmap Epigenomics track hubs on the UCSC Genome Browser. Transcripts are from the GENCODE basic annotation.

Extended Data Table 1 | WHRadjBMI loci with multiple association signals in the sex-combined and/or sex-specific approximate conditional meta-analyses

						Sex-combined			Women			Men			Sex diff.	CEU r^2 with lead
Locus*	SNP	Position (bp)	Nearest gene(s)	EA†	EAF	β	*P*	*N*	β	*P*	*N*	β	*P*	*N*	*P*‡	SNP
TBX15-	rs2645294	119,376,110	*WARS2*	T	0.6	**0.031**	**7.60E-19**	**209,808**	**0.035**	**1.50E-14**	**116,596**	0.014	2.20E-02	93,346	4.90E-03	Same
WARS2	rs1106529	119,333,020	*TBX15*	A	0.8	0.016	1.40E-03	209,930	0.021	1.10E-03	116,663	**0.034**	**4.80E-09**	**93,401**	1.10E-01	0.43
[chr 1]	rs12143789	119,298,677	*TBX15*	C	0.2	**0.026**	**1.00E-09**	**209,874**	0.022	1.30E-04	116,640	0.019	2.30E-03	93,369	7.10E-01	0.06
	rs12731372	118,654,498	*SPAG17*	C	0.8	**0.024**	**1.30E-09**	**209,856**	0.02	1.10E-04	116,636	0.028	3.40E-06	93,354	2.80E-01	>500 kb
GRB14-	rs1128249‖	165,236,870	*COBLL1*	G	0.6	**0.062**	**8.60E-19**	**209,414**	**0.093**	**1.00E-24**	**116,348**	-0.002	7.10E-01	93,200	**8.60E-22**	0.93
COBLL1	rs12692737	165,262,555	*COBLL1*	A	0.3	**0.043**	**1.60E-08**	**203,265**	**0.134**	**2.70E-26**	**112,317**	0.003	5.70E-01	91,082	**2.80E-21**	0.71
[chr 2]	rs12692738	165,266,498	*COBLL1*	T	0.8	0.021	5.90E-05	209,551	**0.092**	**3.80E-20**	**116,474**	-0.005	4.10E-01	93,211	**4.70E-18**	0.3
	rs17185198	165,268,482	*COBLL1*	A	0.8	0.002	7.40E-01	207,702	**0.072**	**8.50E-13**	**115,657**	-0.004	5.80E-01	92,179	**8.00E-11**	0.15
PRBM1	rs13083798	52,624,788	*PRBM1*	A	0.5	**0.023**	**4.10E-11**	**209,128**	0.013	1.20E-01	115,974	0.016	1.10E-03	93,288	7.40E-01	0.88
[chr3]	rs12489828	52,542,054	*NT5DC2*	T	0.6	0.011	6.50E-02	204,485	**0.029**	**2.60E-10**	**112,633**	-0.015	2.90E-03	91,986	**7.20E-11**	0.57
MAP3K1	rs3936510	55,896,623	*MAP3K1*	T	0.2	0.022	1.50E-06	207,896	**0.042**	**6.00E-12**	**115,645**	-0.002	8.20E-01	92,386	**5.90E-07**	0.88
[chr 5]	rs459193	55,842,508	*ANKRD55*	A	0.3	**0.026**	**1.60E-11**	**209,952**	0.016	1.90E-03	116,677	**0.033**	**6.70E-09**	**93,410**	2.30E-02	0.06
VEGFA	rs998584§	43,865,874	*VEGFA*	A	0.5	**0.043**	**1.10E-29**	**189,620**	**0.065**	**1.00E-35**	**106,771**	0.018	8.20E-04	82,983	**3.10E-10**	0.84
[chr 6]	rs4714699	43,910,541	*VEGFA*	C	0.4	0.019	3.50E-07	193,327	**0.028**	**1.00E-08**	**107,987**	0.007	1.90E-01	85,475	4.90E-03	0.01
RSPO3	rs1936805§	127,493,809	*RSPO3*	T	0.5	**0.038**	**2.00E-28**	**209,859**	**0.071**	**6.40E-37**	**116,602**	**0.031**	**3.30E-10**	**93,392**	**8.40E-08**	Same
[chr 6]	rs11961815	127,477,288	*RSPO3*	A	0.8	0.022	5.00E-06	209,679	**0.037**	**6.50E-09**	**116,503**	0.021	3.60E-03	93,310	6.90E-02	0.32
	rs72959041‖	127,496,586	*RSPO3*	A	0.1	**0.101**	**8.70E-15**	**72,472**	-	-	-	-	-	-	-	0.05
NFE2L3,	rs1534696	26,363,764	*SNX10*	C	0.4	0.011	2.00E-03	198,194	**0.028**	**2.00E-08**	**111,643**	-0.007	1.90E-01	86,685	**2.20E-07**	Same
SNX10¶	rs10245353	25,825,139	*NFE2L3*	A	0.2	**0.035**	**8.40E-16**	**210,008**	0.016	1.30E-01	116,704	0.027	1.40E-05	93,438	3.60E-01	Same
[chr 7]	rs3902751	25,828,164	*NFE2L3*	A	0.3	0.009	2.00E-01	209,969	**0.039**	**4.20E-14**	**116,676**	0.019	8.40E-04	93,427	7.40E-03	0.608¶
HOXC13	rs1443512	52,628,951	*HOXC13*	A	0.2	0.016	2.70E-03	209,980	0.04	1.10E-14	116,688	0.012	3.00E-02	93,425	**1.80E-04**	Same
[chr 12]	rs10783615	52,636,040	*HOXC12*	G	0.1	**0.037**	**6.70E-14**	**209,368**	0.023	8.50E-03	116,356	0.022	1.80E-03	93,146	9.30E-01	0.59
	rs2071449§	52,714,278	*HOXC4/5/6*	A	0.4	**0.028**	**5.00E-15**	**206,953**	**0.026**	**4.60E-08**	**114,259**	**0.029**	**3.40E-08**	**92,829**	6.60E-01	0
CCDC92	rs4765219	123,006,063	*CCDC92*	C	0.7	**0.025**	**6.90E-12**	**209,807**	**0.032**	**2.50E-11**	**116,592**	0.018	5.30E-04	93,350	3.80E-02	Same
[chr 12]	rs863750	123,071,397	*ZNF664*	T	0.6	**0.022**	**3.90E-10**	**209,371**	**0.031**	**1.60E-11**	**116,367**	0.015	4.00E-03	93,138	1.80E-02	0.02

P values and β coefficients for the association with WHRadjBMI from the joint model in the approximate conditional analysis of combined GWAS and Metabochip studies. SNPs selected by conditional analyses as independently associated with WHRadjBMI in a meta-analysis (sex-combined, women- or men-specific) have their respective summary statistics for these analyses marked in black and bold. SNPs not selected by a particular conditional analysis as independently associated are marked in grey and show the association analysis results for the SNP conditioned on the locus SNPs selected by GCTA. Sample sizes are from the unconditioned meta-analysis.

* Locus and lead SNPs are defined by Table 1.

† The effect allele is the WHRadjBMI-increasing allele in the sex-combined analysis.

‡ Test for sex difference in conditional analysis based on the effect correlation estimate from primary analyses; values significant at the table-wise Bonferroni threshold of $0.05/25 = 2 \times 10^{-3}$ are marked in bold.

§ SNPs selected by conditional analysis in the sex-combined analysis; proxies were selected by joint conditional analysis in the women- and/or men-specific analyses.

‖ SNP not present in the sex-specific meta-analyses due to sample size filter requiring $n \geq 50{,}000$; sample size from GCTA.

¶ At *NFE2L3-SNX10*, different lead SNPs were identified in the European and all-ancestry analyses but LD is reported with respect to rs10245353.

Extended Data Table 2 | Enrichments of 49 WHRadjBMI signal SNPs with metabolic and anthropometric traits

		SNPs in concordant direction			SNPs in concordant direction with $P < 0.05$		
Trait	Max. sample size	*N*	Total	*P*	*N*	Total	*P*
Type 2 diabetes (T2D)	86,200	37	49	**2.35E-04**	16	49	**3.56E-14**
Fasting glucose (FG)	132,996	35	49	**1.90E-03**	8	49	**2.75E-05**
Fasting insulin adjusted for BMI (FIadjBMI)	103,496	45	49	**4.11E-10**	36	49	**4.04E-47**
2-hour glucose (G120)	42,853	33	49	1.06E-02	7	49	**2.09E-04**
Diastolic blood pressure (DBP)	69,760	34	49	4.70E-03	10	49	**3.21E-07**
Systolic blood pressure (SBP)	69,774	38	49	**7.10E-05**	6	49	**1.36E-03**
Body mass index (BMI)	322,120	40	49	**4.63E-06**	23	49	**4.42E-24**
Height	253,209	25	49	5.00E-01	14	49	**1.10E-11**
High-density lipoprotein cholesterol (HDL-C)	187,142	45	49	**4.11E-10**	24	49	**1.22E-25**
Low-density lipoprotein cholesterol (LDL-C)	173,067	33	49	1.06E-02	12	49	**2.32E-09**
Triglycerides (TG)	177,838	46	49	**3.49E-11**	29	49	**6.02E-34**
Adiponectin	29,347	41	49	**9.82E-07**	20	49	**1.28E-19**
Endometriosis	1,364/7,060	24	45	3.83E-01	4	45	2.58E-02
Nephropathy (in Chinese subjects)	1,194/902	18	43	8.89E-01	0	43	1.00E+00
Nephropathy (in Italian subjects)	1,045/1,340	20	43	7.29E-01	1	43	6.63E-01
Estimated glomerular filtration rate of creatinine (eGFRcrea)	74,354	29	49	1.26E-01	3	49	1.24E-01
Chronic kidney disease (CKD)	74,354	17	49	9.89E-01	2	49	3.47E-01
Urine albumin-to-creatinine ratio (UACR)	31,580	22	49	8.04E-01	2	49	3.47E-01
Menopause	87,802	28	49	1.96E-01	1	49	7.11E-01
Menarche	38,968	23	49	7.16E-01	2	49	3.47E-01
Coronary artery disease (CAD)	191,198	27	48	2.35E-01	9	48	**2.64E-06**
Femoral neck bone mineral density (FN-BMD)	32,960	25	49	5.00E-01	4	49	3.40E-02
Lumbar spine bone mineral density (LS-BMD)	31,798	28	49	1.96E-01	3	49	1.24E-01

The 49 WHRadjBMI SNPs were tested for association with other traits by GWAS meta-analyses performed by other groups (see Methods). The maximum sample size available is shown overall or separately for cases/controls. *N* indicates the number of the total SNPs for which the WHRadjBMI-increasing allele is associated with the trait in the concordant direction (increased levels, except for HDL-C, adiponectin and BMI). One-sided binomial *P* values test whether this number is greater than expected by chance (null $P = 0.5$ and null $P = 0.025$, respectively). The tests do not account for correlation between WHRadjBMI and the tested traits. *P* values representing significant column-wise enrichment ($P < 0.05/23$ tests) are marked in bold.

Extended Data Table 3 | Enrichment of 49 WHRadjBMI-associated loci in epigenomic data sets

Sample	Tissue	DNase I HS	H3K4me1	H3K27ac	H3K4me3	H3K9ac
Adipose Nuclei	Adipose	-	**9.6E-06**	**1.2E-13**	0.0051	0.0010
GM12878	Blood	0.029	0.032	0.32	0.050	0.030
Osteoblasts	Bone	0.082	**4.1E-06**	**1.8E-04**	9.9E-04	-
Astrocytes	Brain	0.013	0.0044	0.0077	0.0047	-
Anterior Caudate	Brain	-	**2.9E-04**	0.026	0.018	0.015
Mid Frontal Lobe	Brain	-	0.029	0.023	0.023	0.036
Substantia Nigra	Brain	-	0.047	-	0.023	0.045
Cerebellum	Brain	0.048	-	-	-	-
Cerebrum Frontal	Brain	0.054	-	-	-	-
Frontal Cortex	Brain	0.022	-	-	-	-
HUVEC	Endothelial	**5.0E-05**	0.011	0.0011	0.023	0.040
Adult Liver	Liver	-	0.0057	-	0.15	0.29
HepG2	Liver	0.015	**7.7E-05**	0.023	**5.0E-04**	0.085
Hepatocytes	Liver	0.59	-	-	-	-
Huh-7	Liver	0.0024	-	-	-	-
Myoctye	Muscle	**2.9E-04**	**1.3E-04**	0.0026	0.015	0.0041
PSOAS	Muscle	0.0012	-	-	-	-
Skeletal Muscle	Muscle	-	**7.3E-04**	**7.8E-05**	0.0075	0.25
Pancreatic Islet	Pancreatic Islets	0.40	0.68	-	0.37	0.61

Enrichment of WHRadjBMI-associated loci in regulatory elements from selected WHRadjBMI-relevant tissues. *P* values are derived using a sum of binomial distributions (see Methods). *P* values below a Bonferroni-corrected threshold for 60 tests of 8.3×10^{-4} are indicated in bold font. The binomial-based *P* values are similar to *P* values generated from 10,000 permutation tests. Dashes indicate that data sets were not available.

Extended Data Table 4 | Candidate genes at new loci associated with additional waist and hip-related traits

SNP	Trait	Chr	Locus	Expression QTL ($P < 10^{-5}$)*	GRAIL ($P < 0.05$)†	Literature‡	Other GWAS signals§	nsSNPs and CNVs ($r^2 > 0.7$)‖
rs10925060	WCadjBMI	1	*OR2W5-NRLP3*	-	-	*NLRP3*	-	-
rs10929925	HIP	2	*SOX11*	-	*SOX11*	*SOX11*	-	-
rs2124969	WCadjBMI	2	*ITGB6*	*PLA2R1* (SAT)	*ITGB6*	-	Idiopathic membranous nephropathy (*PLA2R1, LY75, ITGB6, RBMS1*)	-
rs1664789	WCadjBMI	5	*ARL15*	-	-	*ARL15*	-	-
rs17472426	WCadjBMI	5	*CCNJL*	-	-	*FABP6*	-	-
rs722585	HIPadjBMI	6	*GMDS*	-	-	-	-	-
rs7739232	HIPadjBMI	6	*KLHL31*	*KLHL31* (SAT)	-	*KLHL31-GCLC-ELVOL*	-	-
rs1144	WCadjBMI	7	*SRPK2*	*SRPK2* (LCL), *MLL5* (Omental)	-	-	-	-
rs13241538	HIPadjBMI	7	*KLF14*	*KLF14* (SAT)	-	*KLF14*	HDL cholesterol, Triglycerides, Type 2 diabetes: *KLF14*	-
rs2398893	WHR	9	*PTPDC1*	-	*BARX1*	-	-	-
rs7044106	HIPadjBMI	9	*C5*	-	-	-	-	-
rs11607976	HIP	11	*MYEOV*	-	*CCND1*	*FGF19-FGF4-FGF3*	-	-
rs1784203	WCadjBMI	11	*KIAA1731*	-	-	-	-	-
rs1394461	WHR	11	*CNTN5*	-	-	-	-	-
rs319564	WHR	13	*GPC6*	-	-	*GPC6*	-	-
rs4985155	HIP	16	*PDXDC1*	*PDXDC1* (SAT)	-	*PLA2G10-NTAN1*	Femoral neck bone mineral density, Lumbar spine bone mineral density, Plasma phospholipid levels, Metabolic traits, Height: *PDXDC1, NTAN1*	*NTAN1* (S287P), *NTAN1* (H283N)
rs2047937	WCadjBMI	16	*ZNF423*	-	-	*ZNF423-CNEP1R1*	-	-
rs2034088	HIPadjBMI	17	*VPS53*	*VPS53* (Liver, SAT), *FAM101B* (Omental, SAT)	-	-	-	-
rs1053593	HIPadjBMI	22	*HMGXB4*	*TOM1* (PBMC), *HMGXB4* (Blood, SAT)	-	*HMGXB4*	-	*HMGXB4* (G165V), CNVR8147.1

Candidate genes for loci shown on Table 3 based on secondary analyses or literature review. Further details are provided in other Supplementary Tables and the Supplementary Note. Loci are shown in order of chromosome and position.

* Gene transcript levels associated with SNP genotype (eQTL) in the indicated tissue(s).

† Genes in pathways identified as enriched by GRAIL analysis.

‡ Strongest candidate genes identified based on manual literature review.

§ Traits associated at $P < 5 \times 10^{-8}$ in GWAS lookups or in the GWAS catalogue using the index SNP or a proxy in high LD ($r^2 > 0.7$), and the genes(s) named in those reports.

‖ Non-synonymous variants (nsSNPs) and copy number variants (CNVs) with tag SNPs in high LD with index SNP based on a 1000 Genomes CEU reference panel. DEPICT analysis was not performed for loci associated with these traits.